



17 **Abstract**

18 The phase of precipitation as snow or rain controls numerous hydrologic processes that are
19 fundamental to effective hydrological modeling. Despite its foundational importance to
20 terrestrial hydrology, typical phase prediction methods (PPM) use overly simplistic estimates
21 based on near-surface air temperature. The review conveys the diversity of tools available for
22 PPM in hydrological modeling and the advancements needed to improve predictions in complex
23 terrain characterized by large spatiotemporal variations in precipitation phase. Initially, we
24 review the processes and physics that control precipitation phase as relevant to hydrologists,
25 focusing on the importance of processes occurring aloft. There are a wide range of options for
26 field observations of precipitation phase, but a lack of a robust observation networks in complex
27 terrain. New remote sensing observations have the potential to increase PPM fidelity, but
28 generally require underlying assumptions and field validation before they are operational. We
29 review the types and accuracy of common PPM to show accuracy is generally increased at finer
30 time steps and by including humidity. One important tool for PPM development is atmospheric
31 modeling, which offers numerous models and microphysical schemes that have not been
32 effectively linked to hydrological models or validated against near-surface precipitation phase
33 observations. One important tool for PPM development is atmospheric modeling, which offers
34 numerous models and microphysical schemes that have not been effectively linked to
35 hydrological models or validated against near-surface precipitation phase observations. The
36 review concludes by describing key research gaps and recommendations to improve PPM.
37 Recommendations include incorporate humidity information and atmospheric information into
38 models, develop observation networks at high temporal resolutions, compare and validate
39 different PPM, develop spatially resolved products, and characterize regional variability. PPM is
40 a critical research frontier in hydrology that requires scientific cooperation between hydrological
41 and atmospheric modelers with field hydrologists.

42

43 **Keywords:** precipitation phase, snow, rain, hydrological modeling

44

45 1. Introduction and Motivation

46 As climate warms, a major hydrologic shift in precipitation phase from snow to rain is expected
47 to occur across temperate regions that are reliant on mountain snowpack for water resources
48 (Bales et al., 2006; Barnett et al., 2005). Continued changes in precipitation phase are expected



49 to alter snowpack dynamics and streamflow timing and amounts (Cayan et al., 2001; Fritze et al.,
50 2011; Luce and Holden, 2009; Klos et al., 2014; Berghuijs et al., 2014; Jepsen et al., 2016),
51 increase rain-on snow flooding (McCabe et al., 2007), and challenge our ability to make accurate
52 water supply forecasts (Milly et al., 2008). Accurate estimations of precipitation inputs are
53 required for effective hydrological modeling in both applied and research settings. Snow storage
54 delays the transfer of precipitation into surface runoff and subsurface infiltration (Figure 1),
55 affecting the timing and magnitude of peak flows (Wang et al., 2016), hydrograph recession
56 (Yarnell et al., 2010) and the magnitude and duration of summer baseflow (Safeeq et al., 2014;
57 Godsey et al., 2014). Moreover, the altered timing and rate of snow versus rain inputs can
58 modify the partitioning of water to evapotranspiration versus runoff (Wang et al., 2016).
59 Misrepresentation of precipitation phase within hydrologic models thus propagates into spring
60 snowmelt dynamics (Harder and Pomeroy, 2013; Mizukami et al., 2013; White et al., 2002; Wen
61 et al., 2013) and streamflow estimates used in water resource forecasting. The persistence of
62 streamflow error is particularly problematic for hydrological models that are calibrated on
63 observed streamflow because this error can be compensated for by altering parameters that
64 control other states and fluxes in the model (Minder, 2010; Shamir and Georgakakos,
65 2006; Kirchner, 2006). Expected changes in precipitation phase from climate warming presents a
66 new set of challenges for effective hydrological modeling. A simple yet essential issue for nearly
67 all runoff generation questions is this: Is precipitation falling as rain or snow?

68

69 Despite advances in terrestrial process-representation within hydrological models in the past
70 several decades (Fatichi et al., 2016), the most state-of-the-art models are reliant on simple
71 empirical algorithms to predict precipitation phase. For example, nearly all operational models
72 used by the National Weather Service River Forecast Centers in the United States use some type
73 of temperature-based precipitation-phase partitioning methods (PPM) (Pagano et al., 2014).
74 These are often single or double temperature threshold models that do not consider other
75 conditions important to the hydrometeor's energy balance. Although forcing datasets for
76 hydrological models are rapidly being developed for a suite of meteorological variables, to date
77 no gridded precipitation phase product has been developed over a regional to global scale.
78 Widespread advances in both simulation of terrestrial hydrological processes and computational



79 capabilities may have limited improvements on water resources forecasts without commensurate
80 advances in PPM.

81

82 Recent advances in PPM incorporate effects of humidity (Harder and Pomeroy, 2013; Marks et
83 al., 2013), atmospheric temperature profiles (Froidurot et al., 2014), and remote sensing of phase
84 in the atmosphere (Minder, 2010; Lundquist et al., 2008). A challenge to improving and
85 selecting PPM is the lack of validation data. In particular, reliable ground-based observations of
86 phase are sparse, collected at the point scale over limited areas, and are typically limited to
87 research rather than operational applications (Marks et al., 2013). The lack of observations is
88 particularly problematic in mountain regions where snow-rain transitions are widespread and
89 critical for regional water resource evaluations (Klos et al., 2014). For example, direct visual
90 observations have been widely used (Froidurot et al., 2014; Knowles et al., 2006; U.S. Army
91 Corps of Engineers, 1956), but are decreasing in number in favor of automated measurement
92 systems. Automated systems use indirect methods to accurately estimate precipitation phase
93 from hydrometeor characteristics (i.e. disdrometers), as well as coupled measurements that infer
94 precipitation phase based on multiple lines of evidence (e.g. co-located snow depth and
95 precipitation). Remote sensing is another indirect method that typically uses radar returns from
96 the ground and space-borne platforms to infer hydrometeor temperature and phase. A
97 comprehensive description of the advantages and disadvantages of current measurement
98 strategies, and their correspondence with conventional PPM, is needed to determine critical
99 knowledge gaps and research opportunities.

100

101 New efforts are needed to advance PPM to better inform hydrological models by integrating new
102 observations, expanding the current observation networks, and testing techniques over regional
103 variations in hydroclimatology. While calls to integrate atmospheric information are an
104 important avenue for advancement (Feiccabrino et al., 2012), hydrological models ultimately
105 require accurate and validated phase determination at the land surface. Moreover, any
106 advancement that relies on integrating new information or developing a new PPM technique will
107 require validation and training on ground-based observations. To make tangible advancements
108 in hydrological modeling, new techniques or datasets must be integrated with current modeling
109 tools. The first step towards improved hydrological modeling in areas with mixed precipitation



110 phase is educating the scientific community about current techniques and limitations that point
111 towards knowledge gaps where research is needed.

112

113 This review paper is motivated by a lack of a comprehensive description of the state-of-the-art
114 PPM and observation tools. Therefore, we describe the current state of the science in a way that
115 clarifies the correspondence between techniques and observations and highlights current
116 strengths and weaknesses in the science. Specifically, subsequent sections will review: 1) the
117 processes and physics that control precipitation phase as relevant to field hydrologists, 2) current
118 options available for observing precipitation phase and related measurements common in remote
119 field settings, 3) existing methods for predicting and modeling precipitation phase, and 4)
120 research gaps that exist regarding precipitation phase estimation. The overall objective is to
121 convey a clear understanding of the diversity of tools available for PPM in hydrological
122 modeling and the advancements needed to improve predictions in complex terrain characterized
123 by large spatiotemporal variations in precipitation phase.

124

125 2. Processes and Physics Controlling Precipitation Phase

126 Precipitation is typically formed in the atmosphere as a solid in the mid-latitudes and its phase at
127 the land surface is determined by whether it melts during its fall (Stewart et al., 2015). Most
128 hydrologic models do not simulate atmospheric processes and specify precipitation phase based
129 on surface conditions alone (see Section 4.1), ignoring phase transformations in the atmosphere.

130

131 Several important properties that influence phase changes in the atmosphere are not included in
132 hydrological models (Feiccabrino et al., 2012), such as temperature and precipitation
133 characteristics (Theriault and Stewart, 2010), stability of the atmosphere (Theriault and Stewart,
134 2007), position of the 0 °C isotherm (Minder, 2010; Theriault and Stewart, 2010), interaction
135 between hydrometeors (Stewart, 1992), and the atmospheric humidity profile (Harder and
136 Pomeroy, 2013). The vertical temperature and humidity (represented by the mixing ratio) profile
137 through which the hydrometeor falls typically consists of three layers, a top layer that is frozen
138 ($T < 0\text{ °C}$) in winter in temperate areas (Stewart, 1992), a mixed layer ($T > 0\text{ °C}$), and a surface
139 layer ($T \geq 0\text{ °C}$) (Figure 2). The phase of precipitation at the surface partly depends on the phase
140 reaching the top of the surface layer, which is defined as the critical height. The temperature



141 profile and depth of the surface layer controls the precipitation phase reaching the ground
142 surface. For example, in Figure 2a, if rain reaches the critical height, it may reach the surface as
143 rain or ice pellets depending on small differences in temperature in the surface layer (Theriault
144 and Stewart, 2010). Similarly, in Figure 2b, if snow reaches the critical height, it may reach the
145 surface as snow since the temperature in the surface layer is below freezing. However, in Figure
146 2c, when the surface layer temperatures are close to freezing and the mixing ratios are neither
147 close to saturation or very dry the phase at the surface is not easily determined by the surface
148 conditions alone.

149

150 In addition to strong dependence on the vertical temperature and humidity profiles, precipitation
151 phase is also a function of fall rate and hydrometeor size because they affect energy exchange
152 with the atmosphere (Theriault et al., 2010). Precipitation rate influences the precipitation phase;
153 for example, a precipitation rate of 10 mm h^{-1} reduces the amount of freezing rain by a factor of
154 three over a precipitation rate of 1 mm h^{-1} (Theriault and Stewart, 2010) because there is less
155 time for exchange of turbulent heat with the hydrometeor. A solid hydrometeor that originates in
156 the top layer and falls through the mixed layer can reach the surface layer as wet snow, sleet, or
157 rain. This phase transition in the mixed layer is primarily a function of latent heat exchange
158 driven by vapor pressure gradients and sensible heat exchange driven by temperature gradients.
159 Temperature generally increases from the mixed layer to the surface layer causing sensible heat
160 inputs to the hydrometeor. If these gains in sensible heat are combined with minimal latent heat
161 losses resulting from low vapor pressure deficits, it is likely the hydrometeor will reach the
162 surface layer as rain (Figure 2). However, vapor pressure in the mixed layer is often below
163 saturation leading to latent energy losses and cooling of the hydrometeor coupled with diabatic
164 cooling of the local atmosphere, which can produce snow or other forms of frozen precipitation
165 at the surface even when temperatures are above 0°C . Likewise, surface energetics affect local
166 atmospheric conditions and dynamics, especially in complex terrain. For example, melting of
167 the snowpack can cause diabatic cooling of the local atmosphere and affect the phase of
168 precipitation, especially when air temperatures are very close of 0°C (Theriault et al., 2012).
169 Many conditions lead to a combination of latent heat losses and sensible heat gains by
170 hydrometeors (Figure 2). Under these conditions it can be difficult to predict the phase of



171 precipitation without sufficient information about humidity and temperature profiles, turbulence,
172 hydrometeor size, and precipitation intensity.

173

174 Stability of the atmosphere can also influence precipitation phase. Stability is a function of the
175 vertical temperature structure which can be altered by vertical air movement and hence influence
176 precipitation phase (Theriault and Stewart, 2007). Vertical air velocity changes the temperature
177 structure by adiabatic warming or cooling due to pressure changes of descending and ascending,
178 air parcels, respectively. These changes in temperature will generate under-saturated and
179 supersaturated conditions in the atmosphere that can also alter the precipitation phase. Even very
180 weak vertical air velocity (<10 cm/s) significantly influences the phase and amount of
181 precipitation formed in the atmosphere (Theriault and Stewart, 2007). The rain-snow line
182 predicted by atmospheric models is very sensitive to these microphysics (Minder, 2010).
183 Incorporation and validation of atmospheric microphysics is rarely incorporated in hydrological
184 applications (Feiccabrino et al., 2012).

185

186 3. Current Tools for Observing Precipitation Phase

187 3.1 In situ observations

188 In situ observations refer to methods wherein a person or instrument onsite records precipitation
189 phase. We identify 3 classes of approaches that are used to observe precipitation phase including
190 1) direct observations, 2) coupled observations, and 3) proxy observations.

191

192 Direct observations simply involve a person on-site noting the phase of falling precipitation.
193 Such data form the basis of many of the predictive methods that are widely used (Dai, 2008;
194 Ding et al., 2014; U.S. Army Corps of Engineers, 1956). Direct observations are useful for
195 “manned” stations such as those operated by the U.S. National Weather Service. Few research
196 stations, however, have this benefit, particularly in remote regions. Direct observations are also
197 limited in their temporal resolution and are typically reported only once per day, with some
198 exceptions (Froidurot et al., 2014). Citizen scientist networks have historically provided valuable
199 data to supplement primary instrumented observation networks. The National Weather Service
200 Cooperative Observer Program (<http://www.nws.noaa.gov/om/coop/what-is-coop.html>) is
201 comprised of a network of volunteers recording daily observations of temperature and
202 precipitation, including phase. The NOAA National Severe Storms Laboratory used citizen



203 scientist observations of rain and snow occurrence to evaluate the performance of the Multi-
204 Radar Multi-Sensor (MRMS) system in the meteorological Phenomena Identification Near the
205 Ground (mPING) project (Chen et al., 2015). The Colorado Climate Center initiated Community
206 Collaborative Rain, Hail and Snow Network (CoCoRaHS) supplies volunteers with low cost
207 instrumentation to observe precipitation characteristics, including phase, and enables
208 observations to be reported on the project website (<http://www.cocorahs.org/>). Although highly
209 valuable, some limitations of this system include the imperfect ability of observers to identify
210 mixed phase events and the temporal extent of storms, as well as the lack of observations in both
211 remote areas and during low light conditions.

212

213 Coupled observations link synchronous measurements of precipitation with secondary
214 observations to indicate phase. Secondary observations can include photographs of surrounding
215 terrain, snow depth measurements, and measurements of ancillary meteorological variables.
216 Photographs of vertical scales emplaced in the snow have been used to estimate snow
217 accumulation depth, which can then be coupled with precipitation mass to determine density and
218 phase (Berris and Harr, 1987; Floyd and Weiler, 2008; Garvelmann et al., 2013; Hedrick and
219 Marshall, 2014; Parajka et al., 2012). Mixed phase events, however, are difficult to quantify
220 using coupled depth- and photographic-based techniques (Floyd and Weiler, 2008). Acoustic
221 distance sensors, which are now commonly used to monitor the accumulation of snow (e.g. Boe,
222 2013), have similar drawbacks in mixed phase events, but have been effectively applied to
223 separate snow from rain (Rajagopal and Harpold, 2016). Meteorological information such as
224 temperature and relative humidity can be used to compute the phase of precipitation measured by
225 bucket-type gauges. Unfortunately, this approach generally requires incorporating assumptions
226 about the meteorological conditions that determine phase (see section 4.1). Harder and Pomeroy
227 (2013) used a comprehensive approach to determine the phase of precipitation. Every 15 minutes
228 during their study period phase was determined by evaluating weighing bucket mass, tipping
229 bucket depth, albedo, snow depth, and air temperature. Similarly, Marks et al. (2013) used a
230 scheme based on co-located precipitation and snow depth to discriminate phase. A more
231 involved expert decision making approach by Lejeune et al. (2003) was based on six recorded
232 meteorological parameters: precipitation intensity, albedo of the soil, air temperature, ground
233 surface temperature, reflected long-wave radiation, and soil heat flux. The intent of most of these



234 coupled observations was to develop datasets to evaluate PPM algorithms. However, if these
235 observation systems were sufficiently simple they may have the potential to be applied
236 operationally across larger meteorological monitoring networks (Rajagopal and Harpold, 2016).
237
238 Proxy observations measure geophysical properties of precipitation to infer phase. The hot plate
239 precipitation gauge introduced by Rasmussen et al. (2012), for example, uses a heated thin disk
240 to accumulate precipitation and then measures the amount of energy required to melt snow or
241 evaporate liquid water. This technique, however, requires a secondary measurement of air
242 temperature to determine if the energy is used to melt snow or only evaporate rain. Disdrometers
243 measure the size and velocity of hydrometeors. Although the most common application of
244 disdrometer data is to determine the drop size distribution (DSD) and other properties of rain, the
245 phase of hydrometeors can be inferred by relating velocity and size to density. Some disdrometer
246 technologies, which can be grouped into impact, imaging, and scattering approaches (Loffler-
247 Mang et al., 1999), are better suited for describing snow than others. Impact disdrometers, first
248 introduced by (Joss and Waldvogel, 1967), use an electromechanical sensor to convert the
249 momentum of a hydrometeor into an electric pulse. The amplitude of the pulse is a function of
250 drop diameter. Impact disdrometers have not been commonly used to measure solid precipitation
251 due to the different functional relationships between drop size and momentum for solid and
252 liquid precipitation. Imaging disdrometers use basic photographic principles to acquire images
253 of the distribution of particles (Borrmann and Jaenicke, 1993; Knollenberg, 1970). The 2D Video
254 Disdrometer (2DVD) described by Kruger and Krajewski (2002) records the shadows cast by
255 hydrometeors onto photodetectors as they pass through two sheets of light. The shape of the
256 shadows enables computation of particle size, and shadows are tracked through both light sheets
257 to determine velocity. Although initially designed to describe liquid precipitation, recent work
258 has shown that the 2DVD can be used to classify snowfall according to microphysical properties
259 of single hydrometeors (Bernauer et al., 2016). The 2DVD has been used to classify known rain
260 or snow events individually, but little work has been performed to distinguish between liquid and
261 solid precipitation. Scattering disdrometers, or optical disdrometers, measure the extinction of
262 light passing between a source and a sensor (Hauser et al., 1984; Loffler-Mang et al., 1999). Like
263 the other types, optical disdrometers were originally designed for rain, but have been periodically
264 applied to snow (Battaglia et al., 2010; Lempio et al., 2007). In a comparison study, the



265 PARSIVEL optical disdrometer, originally described by Löffler-Mang et al. (1999) did not
266 perform well against a 2DVD because of problems related to the detection of slow fall velocities
267 for snow. It may be possible to use optical disdrometers to distinguish between rain, sleet, and
268 snow based on the existence of distinct shapes of the size spectra for each precipitation type.
269 More research on the relationship between air temperature and the size spectra produced by the
270 optical disdrometer is needed (Lempio et al., 2007). In summary, disdrometers of various types
271 are valuable tools for describing the properties of rain and snow, but require further testing and
272 development to distinguish between rain and snow, as well as mixed phase events.

273

274 3.2 Ground-based remote sensing observations

275 Until recently, most ground-based radar stations were operated as conventional Doppler systems
276 that transmit and receive radio waves with single horizontal polarization. Developments in dual
277 polarization ground radar such as those that function as part of the U.S. National Weather
278 Service NEXRAD network, have resulted in systems that transmit radio signals with both
279 horizontal and vertical polarizations. This section will review techniques for determining
280 precipitation phase used with data from single- and dual-pol systems.

281

282 Ground-based remote sensing of precipitation phase using single-polarized radar systems
283 depends on detecting the radar bright band. Radio waves transmitted by the radar system, are
284 scattered by hydrometeors in the atmosphere, with a certain proportion reflected back towards
285 the radar antenna. The magnitude of the measured reflectivity (Z) is related to the size and the
286 dielectric constant of falling hydrometeors (White et al., 2002). Ice particles aggregate as they
287 descend through the atmosphere and their dielectric constant increases, in turn increasing Z
288 measured by the radar, creating the bright band, a layer of enhanced reflectivity just below the
289 elevation of the melting level (Lundquist et al., 2008). Therefore, bright band elevation can be
290 used as a proxy for the “snow level”, the bottom of the melting layer where falling snow
291 transforms to rain (White et al., 2010; White et al., 2002).

292

293 Doppler vertical velocity (DVV) is another variable that can be estimated from single-polarized
294 radar. It is derived from vertically profiling radars. DVV gives an estimate of the velocity of
295 falling particles; as snowflakes melt and become liquid raindrops, the fall velocity of the altered



296 hydrometeors increases. When combined with reflectivity profiles, DVV helps reduce false
297 positive detection of the bright band, which may be caused by phenomena other than snow
298 melting to rain (White et al., 2002). First, DVV and Z are combined to detect the elevation of the
299 bottom of the bright band. Then the algorithm searches for maximum Z above the bottom of the
300 bright band and determines that to be the bright band elevation (White et al., 2002). However, a
301 test of this algorithm on data from a winter storm over the Sierra Nevada found root mean square
302 errors of 326 to 457 m compared to ground observations when bright band elevation was
303 assumed to represent the surface transition from snow to rain [Lundquist et al., 2008]. Snow
304 levels in mountainous areas, however, may also be overestimated by radar profiler estimates if
305 they are unable to resolve spatial variations close to mountain fronts, since snow levels have
306 been noted to persistently drop on windward slopes (Minder and Kingsmill, 2013). Despite the
307 potential errors, the elevation of maximum Z may be a useful proxy variable for snow level in
308 hydrometeorological applications in mountainous watersheds because maximum Z will always
309 occur below the freezing level (White et al., 2010;Lundquist et al., 2008)

310

311 Few published studies have explored the value of bright band-derived phase data for hydrologic
312 modeling. Maurer and Mass (2006) compared the melting level from vertically pointing radar
313 reflectivity against temperature-based methods to assess whether the radar approach could
314 improve determination of precipitation phase at the ground level. In that study, the altitude of the
315 top of the bright band was detected and applied across the study basin. Frozen precipitation was
316 assumed to be falling in model pixels above the altitude of the melting level and liquid
317 precipitation was assumed to be falling in pixels below the altitude of the melting layer (Maurer
318 and Mass, 2006). Maurer and Mass (2006) found that incorporating radar-detected melting layer
319 altitude improved streamflow simulation results. A similar study that used bright band altitude to
320 classify pixels according to surface precipitation type was not as conclusive; bright band altitude
321 data did not improve hydrologic model simulation results over those based on a temperature
322 threshold (Mizukami et al., 2013). Also, the potential of the method is limited to the availability
323 of vertically pointing radar; in complex, mountainous terrain the ability to estimate melting level
324 becomes increasingly challenging with distance from the radar.

325



326 Dual-polarized radar systems generate more variables than traditional single-polarized systems.
327 These polarimetric variables include differential reflectivity (Z_{DR}), reflectivity difference (Z_{DP}),
328 the correlation coefficient (ρ_{nv}), and specific differential phase (K_{DP}). Polarimetric variables
329 respond to hydrometeor properties such as shape, size, orientation, phase state, and fall behavior
330 and can be used to assign hydrometeors to specific categories (Chandrasekar et al., 2013; Grazioli
331 et al., 2015), or to improve bright band detection (Giangrande et al., 2008).

332

333 Various hydrometeor classification algorithms have been applied to X-, C- and S-band
334 wavelengths. Improvements in these algorithms over recent years have seen hydrometeor
335 classification become an operational meteorological product (see Grazioli et al., 2015 for an
336 overview). For example, the U.S. National Severe Storms Laboratory (NSSL) developed a fuzzy-
337 logic hydrometeor classification algorithm for warm-season convective weather (Park et al.,
338 2009) and this algorithm has also been tested for cold-season events (Elmore, 2011). Its skill
339 was tested against surface observations of precipitation type but it was found that the algorithm
340 did not perform well in classifying winter precipitation because it could not account for re-
341 freezing of hydrometeors below the melting level (Elmore, 2011). Unlike warm season
342 convective precipitation, the freezing level during a cold-season precipitation event can vary
343 spatially. This phenomenon has prompted the use of polarimetric variables to first detect the
344 melting layer, and then classify hydrometeors (Boodoo et al., 2010; Thompson et al., 2014).
345 Although there has been some success in developing two-stage cold-season hydrometeor
346 classification algorithms, there is little in the published literature that explores the potential
347 contributions of these algorithms for partitioning snow and rain for hydrological modeling.

348

349 3.3 Space-based remote sensing observations

350 Passive microwave radiometers detect microwave radiation emitted by the Earth's surface or
351 atmosphere. Passive microwave remote sensing has potential for discriminating between rainfall
352 and snowfall because microwave radiation emitted by the Earth's surface propagates through all
353 but the densest precipitating clouds, meaning that radiation at microwave wavelengths directly
354 interacts with hydrometeors within clouds (Olson et al., 1996; and Ardanuy, 1989). However,
355 the remote sensing of precipitation in microwave wavelengths and the development of
356 operational algorithms is dominated by research focused on rainfall (Arkin and Ardanuy, 1989);



357 by comparison, snowfall detection and observation has received less attention (Noh et al., 2009;
358 Kim et al., 2008). This is partly explained by examining the physical processes within clouds that
359 attenuate the microwave signal. Raindrops emit low levels of microwave radiation increasing the
360 level of radiance measured by the sensor; in contrast, ice hydrometeors scatter microwave
361 radiation, decreasing the radiance measured by a sensor (Kidd and Huffman, 2011). Land
362 surfaces have a much higher emissivity than water surfaces, meaning that emission-based
363 detection of precipitation is challenging over land because the high microwave emissions mask
364 the emission signal from raindrops (Kidd, 1998; Kidd and Huffman, 2011). Thus, scattering-
365 based techniques using medium to high frequencies are used to detect precipitation over land.
366 Moreover, microwave observations at higher frequencies (> 89 GHz) have been shown to
367 discriminate between liquid and frozen hydrometeors (Wilheit et al., 1982).

368

369 Retrieving snowfall over land areas from spaceborne microwave sensors can be even more
370 challenging than for liquid precipitation because existing snow cover increases microwave
371 emission. Depression of the microwave signal caused by scattering from ice particles may be
372 obscured by increased emission of microwave radiation from the snow covered land surface.
373 Kongoli et al. (2003) demonstrated an operational snowfall detection algorithm that accounts for
374 the problem of existing snow cover. This group used data from the Advanced Microwave
375 Sounding Unit-A (AMSU-A), a 15-channel atmospheric temperature sounder with a single high
376 frequency channel at 89 GHz, and AMSU-B, a 5-channel high frequency microwave humidity
377 sounder. Both sensors were mounted on the NOAA-16 and -17 polar-orbiting satellites. While
378 the algorithm worked well for warmer, opaque atmospheres, it was found to be too noisy for
379 colder, clear atmospheres. Additionally, some snowfall events occur under warmer conditions
380 than those that were the focus of the study (Kongoli et al., 2003). Kongoli et al. (2015) further
381 adapted their methodology for the Advanced Technology Microwave Sounder (ATMS), onboard
382 the polar-orbiting Suomi National Polar-orbiting Partnership satellite, a descendant of the AMSU
383 sounders. The latest algorithm assesses the probability of snowfall using the logistic regression
384 and the principal components of seven high frequency bands at 89 GHz and above. In testing, the
385 Kongoli et al. (2015) algorithm has shown skill in detecting snowfall both at variable rates and
386 when snowfall is lighter and occurs in colder conditions. An alternative algorithm by Noh et al.,
387 2009 used physically-based, radiative transfer modeling in an attempt to improve snowfall



388 retrieval over land. In this case, radiative transfer modeling was used to construct an *a priori*
389 database of observed snowfall profiles and corresponding brightness temperatures. The radiative
390 transfer procedure yields likely brightness temperatures from modeling how ice particles scatter
391 microwave radiation at different wavelengths. A Bayesian retrieval algorithm was then used to
392 estimate snowfall over land by comparing measurements of brightness temperature with modeled
393 brightness temperature (Noh *et al.*, 2009). The algorithm was tested during the early and late
394 winter for heavier snowfall events. Late winter retrievals indicated that the algorithm
395 overestimated snowfall, over surfaces with significant snow accumulation.

396

397 While results have been promising, the spatial resolution at which ATMS and other passive
398 microwave data are acquired is very coarse (15.8 to 74.8 km at nadir), making passive
399 microwave approaches more applicable for regional to continental scales. Temporal resolution of
400 the data acquisition is another challenge. AMSU instruments are mounted on 8 satellites; the
401 related ATMS is mounted on a single satellite and planned for two additional satellites. However,
402 the satellites are polar-orbiting, not geostationary, so it is probable that a precipitation event
403 could occur outside the field of view of one of the instruments.

404

405 Spaceborne active microwave or radar sensors measure the backscattered signal from pulses of
406 microwave energy emitted by the sensor itself. Much like the ground based radar systems, the
407 propagated microwave signal interacts with liquid and solid particles in the atmosphere and the
408 degree to which the measured return signal is attenuated provides information on the
409 atmospheric constituents. The advantage offered by spaceborne radar sensors over passive
410 microwave is the capability to acquire more detailed sampling of the vertical profile of the
411 atmosphere (Kulie and Bennartz, 2009). The first spaceborne radar capable of observing
412 snowfall is the Cloud Profiling Radar (CPR) onboard CloudSat (2006 – present). The CPR
413 operates at 94 GHz with an along-track (or vertical) resolution of ~1.5 km. Retrieval of dry
414 snowfall rate from CPR measurements of reflectivity have been shown to correspond with
415 estimates of snowfall from ground-based radar at elevations of 2.6 and 3.6 km above mean sea
416 level (Matrosov *et al.*, 2008). Estimates at lower elevations, especially those in the lowest 1 km,
417 are contaminated by ground clutter. Alternative approaches, combining CPR data with ancillary
418 data have been formulated to account for this challenge (Liu 2008; Kulie and Bennartz, 2009).



419 Known relationships between CPR reflectivity data and the scattering properties of non-spherical
420 ice crystals are used to derive snowfall at a given elevation above mean sea level; below this
421 elevation a temperature threshold derived from surface data is used to discriminate between rain
422 and snow events. Liu (2008) used <2 °C as the snow/rain threshold, whereas Kulie and Bennartz
423 (2009) used 0 °C as the snow/rain threshold. Despite the fact that temperature thresholds are
424 incorporated into these latter approaches, they have been the subject of much research and debate
425 for discriminating precipitation phase, as is further discussed in section 4.1.

426

427 CloudSat is part of the A-train or afternoon constellation of satellites, which includes Aqua, with
428 the Moderate Resolution Imaging Spectrometer (MODIS) and the Cloud–Aerosol Lidar and
429 Infrared Pathfinder Satellite Observations (CALIPSO) spacecraft with cloud-profiling Lidar. The
430 sensors onboard A-train satellites provided the unique combination of data to create an
431 operational snow retrieval product. The CPR Level 2 snow profile product (2C-SNOW-
432 PROFILE) uses vertical profile data from the CPR, input from MODIS and the cloud profiling
433 radar, as well as weather forecast data to estimate near surface snowfall (Wood et al., 2013;Kulie
434 et al., 2016). The performance of 2C-SNOW-PROFILE was tested by Cao et al. (2014). This
435 group found the product worked well in detecting light snow but performed less satisfactorily
436 under conditions of moderate to heavy snow because of the non-stationary effects of attenuation
437 on the returned radar signal.

438

439 The launch of the Global Precipitation Mission core observatory in February 2014 holds promise
440 for the future deployment of operational snow detection products. Building on the success of the
441 Tropical Rainfall Monitoring Mission (TRMM), the GPM core observatory sensors include
442 precipitation radar (DPR) and microwave imager (GMI). The GMI has two millimeter wave
443 channels (166 and 183 GHz) that are specifically designed to detect and retrieve light rain and
444 snow precipitation. These are more advanced than the sensors onboard the TRMM spacecraft
445 and permit better quantification of the physical properties of precipitating particles, particularly
446 over land at middle to high latitudes (Hou et al., 2014). Algorithms for the GPM mission are still
447 under development, and is partly being driven by data collected during the GPM Cold Season
448 Experiment (GCPEX) (Skofronick-Jackson et al., 2015). Using airborne sensors to simulate GPM
449 and DPR measurements, one of the questions that the GCPEX hoped to address concerned the



450 potential capability of data from the DPR and GMI to discriminate falling snow from rain or
451 clear air (Skofronick-Jackson et al., 2015). The initial results reported by the GCPEX study echo
452 some of the challenges recognized for ground-based single polarized radar detection of snowfall.
453 The relationship between radar reflectivity and snowfall is not unique. For the GPM mission, it
454 will be necessary to include more variables from dual frequency radar measurements, multiple
455 frequency passive microwave measurements, or a combination of radar and passive microwave
456 measurements (Skofronick-Jackson et al., 2015).

457

458 4. Current Tools for Predicting Precipitation Phase

459 4.1 Prediction Techniques from Ground-Based Observations

460 Discriminating between solid and liquid precipitation is often based on a near-surface air
461 temperature threshold (Martinec and Rango, 1986; U.S. Army Corps of Engineers, 1956; L'hôte et
462 al., 2005). Four prediction methods have been developed that use near-surface air temperature
463 for discriminating precipitation phase: 1) static threshold, 2) linear transition, 3) minimum and
464 maximum temperature, and 4) sigmoidal curve (Table 1). A static temperature threshold applies
465 a single temperature value, such as mean daily temperature, where all of the precipitation above
466 the threshold is rain, and all below that threshold is snow. Typically this threshold temperature is
467 near 0 °C (Motoyama, 1990; Lynch-Stieglitz, 1994), but was shown to be highly variable across
468 both space and time (Kienzle, 2008; Motoyama, 1990; Braun, 1984; Ye et al., 2013a). For
469 example, Rajagopal and Harpold (2016) optimized a single temperature threshold at Snow
470 Telemetry sites across the Western U.S. to show regional variability from -4 to 3 °C (Figure 3).
471 A second discrimination technique is to linearly scale the proportion of snow and rain between a
472 temperature for all rain (T_{rain}) and a temperature for all snow (T_{snow}) (Pipes and Quick,
473 1977; McCabe and Wolock, 2010; Tarboton et al., 1995). Linear threshold models have been
474 parameterized slightly differently across studies, e.g.: $T_{\text{snow}} = -1.0$ °C, $T_{\text{rain}} = 3.0$ °C (McCabe and
475 Wolock, 2010), $T_{\text{snow}} = -1.1$ °C and $T_{\text{rain}} = 3.3$ °C (Tarboton et al., 1995), and $T_{\text{snow}} = 0$ °C and T_{rain}
476 $= 5$ °C (McCabe and Wolock, 1999). A third technique specifies a threshold temperature based
477 on daily minimum and maximum temperatures to classify rain and snow, respectively, with a
478 threshold temperature between the daily minimum and maximum producing a proportion of rain
479 and snow (Leavesley et al., 1996). This technique can have a time-varying temperature
480 threshold or include a T_{rain} that is independent of daily maximum temperature. A fourth



481 technique applies a sigmoidal relationship between mean daily (or sub daily) temperature and the
482 proportion or probability of snow versus rain. For example, one method derived for southern
483 Alberta, Canada employs a curvilinear relationship defined by two variables, a mean daily
484 temperature threshold where 50% of precipitation is snow, and a temperature range where
485 mixed-precipitation can occur (Kienzle, 2008). Another sigmoidal-based empirical model
486 identified a hyperbolic tangent function defined by four parameters to estimate the conditional
487 snow (or rain) frequency based on a global analysis of precipitation phase observations from
488 over 15,000 land-based stations (Dai, 2008). Selection between temperature-based techniques is
489 typically based on available data, with a limited number of studies quantifying their relative
490 accuracy for hydrological applications (Harder and Pomeroy, 2014).

491

492 Several studies have compared the accuracy of temperature-based PPM to one another and/or
493 against an independent validation of precipitation phase. Sevruk (1984) found that only about
494 68% of the variability in monthly observed snow proportion in Switzerland could be explained
495 by threshold temperature based methods near 0 °C. An analysis of data from fifteen stations in
496 southern Alberta, Canada with an average of >30 years of direct observations noted over-
497 estimations in the mean annual snowfall for static threshold (8.1%), linear transition (8.2%),
498 minimum and maximum (9.6%), and sigmoidal transition (7.1%) based methods (Kienzle, 2008).
499 An evaluation of PPM at three sites in the Canadian Rockies by Harder and Pomeroy (2013)
500 found the largest percent error to occur using a static threshold (11% to 18%), followed by linear
501 relationships (-8% to 11%), followed by a sigmoidal relationships (-3 to 11%). Another study
502 using 824 stations in China with >30 years of direct observations found accuracies of 51.4%
503 using a static 2.2 °C threshold and 35.7% to 47.4% using linear temperature-based thresholds
504 (Ding et al., 2014). Lastly, for multiple sites across the rain-snow transition in southwestern
505 Idaho, static temperature thresholds produced the lowest proportion (68%) whereas a linear-
506 based model produced the highest proportion (75%) of snow, respectively (Marks et al., 2013).
507 Generally these accuracy assessments demonstrated that static threshold methods produced the
508 greatest errors, whereas sigmoidal relationships produced the smallest errors, although variations
509 to this general rule existed across sites.

510



511 Near surface humidity also influences precipitation phase (see Section 2). Three humidity-
512 dependent precipitation phase identification methods are found in the literature: 1) dewpoint
513 temperature (T_d), 2) wet bulb temperature (T_w), and 3) psychrometric energy balance. The
514 dewpoint temperature is the temperature at which an air parcel with a fixed pressure and
515 moisture content would be saturated. In one approach to account for measurement and
516 instrument calibration uncertainties of ± 0.25 °C each, T_d and T_w below -0.5 °C was assumed to
517 be all snow and above $+0.5$ °C all rain, with a linear relationship between the two being a
518 proportional mix of snow and rain (Marks et al., 2013). T_d of 0.0 °C performed consistently
519 better than T_a in one study by Marks et al. (2001) while a T_d of 0.1 °C for multiple stations in
520 Sweden was less accurate than a T_a of 1.0 °C (Feiccabrino et al., 2013). The wet or ice bulb
521 temperature (T_w) is the temperature at which an air parcel would become saturated by
522 evaporative cooling in the absence of other sources of sensible heat, and is the lowest
523 temperature that falling precipitation can reach. Few studies have investigated the feasibility of
524 T_w for precipitation phase prediction (Olsen, 2003; Ding et al., 2014; Marks et al., 2013). T_w
525 significantly improved prediction of precipitation phase over T_a at 15-minute time steps, but only
526 marginally improved prediction at daily time steps (Marks et al., 2013). Ding et al. (2014)
527 developed a sigmoidal phase probability curve based on T_w and elevation that outperformed T_a
528 threshold-based methods across a network of sites in China. Conceptually, the hydrometeor
529 temperature (T_i) is similar to T_w but is calculated using the latent heat and vapor density gradient.
530 Use of computed T_i value significantly improved precipitation phase estimates over T_a ,
531 particularly as time scales approached one day (Harder and Pomeroy, 2013).

532

533 There has been limited validation of humidity-based precipitation phase prediction techniques
534 against ground-truth observations. Ding et al. (2014) showed that a method based on T_w and
535 elevation increased accuracy by 4.8% to 8.9% over several temperature-based methods. Their
536 method was more accurate than a simpler T_w based method by (Yamazaki, 2001). Feiccabrino et
537 al. (2013) showed that T_d misclassified 3.0% of snow and rain (excluding mixed phased
538 precipitation), whereas T_a only misclassified 2.4%. Ye et al. (2013b) found T_d less sensitive to
539 phase discrimination under diverse environmental conditions and seasons than T_a . Frudoiret et
540 al. (2014) evaluated several techniques with a critical success index (CSI) at sites across
541 Switzerland to show the highest CSI were associated with variables that included T_w or relative



542 humidity (CSI=84%-85%) compared to T_a (CSI=78%). Marks et al. (2013) evaluated the time at
543 which phase transitioned from snow to rain against field observations across a range of
544 elevations and found that T_d most closely predicted the timing of phase change, whereas both T_a
545 and T_w estimated earlier phase changes than observed. Harder and Pomeroy (2013) compared T_i
546 with field observations and found that error was <10% when T_i was allowed to vary with each
547 daily time-step and >10% when T_i was fixed at 0 °C. The T_i accuracy increased appreciably (i.e.
548 5%-10% improvement) when the temporal resolution was decreased from daily to hourly or 15-
549 minute time steps. The validation studies consistently showed improvements in accuracy by
550 including humidity over PPM based only on temperature.

551

552 Hydrological models employ a variety of techniques for phase prediction using ground based
553 observations (Table 1). All discrete hydrological models (i.e. not coupled to an atmospheric
554 model) investigated used temperature based thresholds that did not consider the near-surface
555 humidity. Moreover, most models use a single static temperature threshold, which was
556 consistently shown to produce lower accuracy than multiple temperature methods. Hydrological
557 models that are coupled to atmospheric models were more able to consider important controls on
558 precipitation phase, such as humidity and atmospheric profiles. This compendium of model
559 PPM highlights the current shortcomings in phase prediction in conventional discrete
560 hydrological models.

561

562 4.2 Prediction Techniques Incorporating Atmospheric Information

563 While many hydrologic models have their own formulations for determining precipitation phase
564 at the ground, it is also possible to initialize hydrologic models with precipitation phase fraction,
565 intensity, and volume from numerical weather simulation model output. Here we discuss the
566 limitations of precipitation phase simulation inherent to WRF (Kaplan et al., 2012; Skamarock et
567 al., 2008) and other atmospheric simulation models. The finest scale spatial resolution employed
568 in atmospheric simulation models is ~1 km and these models generate data at hourly or finer
569 temporal resolutions. Regional climate models (RCM) and global climate models (GCM) are
570 typically coarser than local mesoscale models. The physical processes driving both the removal
571 of moisture from the air and the precipitation phase (Section 2) occur at much finer spatial and
572 temporal resolutions in the real atmosphere than models typically resolve, i.e. <1 km. As with all



573 numerical models, the representation of sub-grid scale processes requires parameterization. At
574 typical scales considered, characterization of mixed phase processes within a condensing cloud
575 depends on both cloud microphysics and kinematics of the surrounding atmosphere. Replicating
576 cloud physics at the multi-kilometer scale requires empiricism. The 30+ cloud microphysics
577 parameterization options in the research version of WRF (Skamarock et al., 2008) vary in the
578 number of classes described (cloud ice, cloud liquid, snow, rain, graupel, hail, etc.), and may or
579 may not accurately resolve changes in hydrometeor phase and horizontal spatial location (due to
580 wind) during precipitation. All microphysical schemes predict cloud water and cloud ice based
581 on internal cloud processes that include a variety of empirical formulations or even simple
582 lookup tables. These schemes vary greatly in their accuracy with “mixed phase” schemes
583 generally performing the best (Lin, 2007; Reisner et al., 1998; Thompson et al., 2004; Thompson
584 et al., 2008; Morrison et al., 2005; Zängl, 2007). For example, the autoconversion and growth
585 processes from cloud water or ice to hydrometeors contain a strong component of empiricism, in
586 particular the nucleation media and their chemical composition. Different microphysical
587 parameterizations lead to different spatial distributions of precipitation and produce varying
588 vertical distributions of hydrometeors (Gilmore et al., 2004). Regardless, precipitation rates for
589 each grid cell are averages requiring hydrological modelers to consider the effects of elevation,
590 aspect, etc. in resolving precipitation phase fractions for finer-scale models.

591

592 Numerical models that contain sophisticated cloud microphysics schemes allow assimilation of
593 additional remote sensing data beyond conventional synoptic/large scale observations (balloon
594 data). This is because the coarse spatial and temporal nature of radiosonde data results in the
595 atmosphere being sensed imperfectly/incompletely compared with the scale of motion that
596 weather simulation models can numerically resolve. These observational inadequacies are
597 exacerbated in complex terrain, where precipitation phase fractions can vary on small scales but
598 radar can be blocked by topography and therefore rendered useless in the model initialization.
599 Accurate generation of liquid and frozen precipitation from vapor requires accurate depiction of
600 initial atmospheric moisture conditions (Kalnay and Cai, 2003; Lewis et al., 2006). In
601 acknowledgement of the difficulty and uncertainty of initializing numerical simulation models,
602 atmospheric modelers use the term “bogusing” to describe incorporation of individual
603 observations at a point location into large scale initial conditions in an effort to enhance the



604 accuracy of the simulation (Eddington, 1989). They also employ complex assimilation
605 methodologies to force the early period of the model solutions during the time integration
606 towards fine scale observations (Kalnay and Cai, 2003; Lewis et al., 2006). These asynoptic or
607 fine scale data sources often substantially improve the accuracy of the simulations as time
608 progresses.

609

610 Hydrologists are increasingly using output from atmospheric models to drive hydrologic models
611 from daily to climate or multi-decadal timescales (Tung and Haith, 1995; Pachauri, 2002; Wood
612 et al., 2004; Rojas et al., 2011; Yucel et al., 2015). These atmospheric models suffer from the
613 same data paucity and scale issues that likewise challenge the implementation and validation of
614 hydrologic models. Uncertainties in their output, including precipitation volume and phase,
615 begins with the initialization of the atmospheric model from measurements, increases with model
616 choice and microphysics as well as turbulence parameterizations, and is a strong function of the
617 scale of the model. The significance of these uncertainties varies by application, but should be
618 acknowledged. Furthermore, these uncertainties are highly variable in character and magnitude
619 from day to day and location to location. Thus, there has been very little published concerning
620 how well atmospheric models predict precipitation phase. Finally, lack of ground measurements
621 leaves the hydrologist no means to assess and validate atmospheric model predictions.

622

623 5. Research Gaps

624 Meeting the challenge of accurately predicting precipitation phase requires the closing of several
625 critical research gaps. Perhaps the most pressing challenge for improving PPM is developing
626 and employing new and improved sources of data. However, new data sources will not yield
627 much benefit without effective incorporation of data into predictive models. Additionally, both
628 the scientific and management communities lack data products that can be readily understood
629 and broadly used. Addressing these research gaps requires simultaneous engagement both
630 within and between the hydrology and atmospheric observation and modeling communities.
631 Changes to atmospheric temperature and humidity profiles from regional climate change will
632 likely challenge conventional precipitation phase prediction in ways that demand additional
633 observations and improved forecasts.

634



635 5.1 Incorporate humidity information

636 Atmospheric humidity affects the energy budget of falling hydrometeors (Section 4.1), but is
637 rarely considered in precipitation phase prediction. The difficulty in incorporating humidity
638 mainly arises from a lack of observations, both as point measurements and distributed gridded
639 products. For example, while some reanalysis products have humidity information (i.e. National
640 Centers for Environmental Prediction, NCEP reanalysis) they are at spatial scales (i.e. > 1
641 degree) to coarse for resolving precipitation phase in complex topography. Addition of high-
642 quality aspirated humidity sensors at snow monitoring stations, such as the SNOTEL network,
643 would advance our understanding of humidity and its effects on precipitation phase in the
644 mountains. Because dry air masses have regional variations controlled by storm tracks and
645 proximity to water bodies, sensitivity of precipitation phase to humidity variations driven by
646 regional warming remains relatively unexplored.

647

648 Although humidity datasets are relatively rare in mountain environments, some gridded data
649 products exist that can be used to investigate the importance of humidity information. Most
650 interpolated gridded data products either do not include any measure of humidity (i.e. Daymet or
651 WorldClim) or use daily temperature measurements to infer humidity conditions (i.e. PRISM).
652 Potentially more useful are data assimilation products, such as NLDAS-2, that provide humidity
653 and temperature values at 1/8th of a degree scale over the continental U.S. In addition, several
654 data reanalysis products are often available at 1 to 3 year lags from present, including
655 NCEP/NCAR, NARR, and the 20th Century reanalysis. Given the relatively sparse observations
656 of humidity in mountain environments, the accuracy of gridded humidity products is rarely
657 rigorously evaluated (Abatzoglou, 2013). More work is needed to understand the added skill
658 provided by humidity datasets for predicting precipitation phase and its distribution over time
659 and space.

660

661 5.2 Incorporate atmospheric information

662 We echo the call of Feiccabrino et al. (2012) for greater incorporation of atmospheric
663 information into phase prediction and additional verification of the skill in phase prediction
664 provided by atmospheric information.

665



666 Several avenues exist to better incorporate atmospheric information into precipitation phase
667 prediction, including direct observations, remote sensing observations, and model products.
668 Radiosonde measurements made daily at many airports and weather forecasting centers have
669 shown some promise for supplying atmospheric profiles of temperature and humidity (Froidurot
670 et al., 2014). However, these data are only useful to initialize the larger scale structure of water
671 vapor and it is their lack of temporal and spatial frequency that prevents their use in accurate
672 precipitation phase prediction, which is inherently a mesoscale problem, i.e., scales of motion
673 <100 km. Atmospheric information on the bright-band height from Doppler radar has been
674 utilized for predicting the altitude of the rain-snow transition (Lundquist et al., 2008;Minder,
675 2010), but has rarely been incorporated into hydrological modeling applications (Maurer and
676 Mass, 2006; Mizukami et al., 2013). In addition to atmospheric observations, modeling products
677 that assimilate observations or are fully physically-based may provide additional information for
678 precipitation phase prediction. Numerous reanalysis products (described in Section 2.2) provide
679 temperature and humidity at different pressure levels within the atmosphere. To our knowledge,
680 information from reanalysis products has yet to be incorporated into precipitation phase
681 prediction for hydrological applications. Bulk microphysical schemes used by meteorological
682 models (i.e. Weather Research and Forecasting WRF model) provide a physically-based estimate
683 of precipitation phase. These schemes capture a wide-variety of processes, including
684 evaporation, sublimation, condensation, and aggradation, and output between two and ten
685 precipitation types. Reduced computational restrictions on running these models over large
686 geographic extents (Rasmussen et al., 2012) are enabling further investigations into precipitation
687 phase change under historical and future climate scenarios. A potentially impactful area of
688 research is to integrate this information into novel approaches to improve precipitation phase
689 prediction skill.

690

691 5.3 Disdrometer networks operating at high temporal resolutions

692 An increase in the types and reliability of disdrometers over the last decade has provided a new
693 suite of tools to more directly measure precipitation phase. Despite this new potential resource
694 for distinguishing snow and rain, very limited deployments of disdrometers have occurred at the
695 scale necessary to improve hydrologic modeling and rain-snow elevation estimates. The lack of
696 disdrometer deployment likely arises from a number of potential limitations: 1) known issues



697 with accuracy, 2) cost of these systems, and 3) power requirements needed for heating elements.
698 These limitations are clearly a factor in procuring large networks and deploying disdrometers in
699 remote areas. However, we advise that disdrometers offer numerous benefits that cannot be
700 substituted with other measurements: 1) they operate at fine temporal scales, 2) they operate in
701 low light conditions that limit other direct observations, and 3) they provide land surface
702 observations rather than precipitation phase in the atmosphere (as compared to more remote
703 methods). Moreover, improvements in disdrometer and power supply technologies that address
704 these limitations would remove restrictions on increased disdrometer deployment.

705

706 Transects of disdrometers spanning the rain-snow elevations of key mountain areas could add
707 substantially to both prediction of precipitation phase for modeling purposes, as well as
708 validating typical predictive models. We advocate for transects over key mountain passes where
709 power is generally available and weather forecasts for travel are particularly important. In
710 addition, co-locating disdrometers at long-term research stations where precipitation phase
711 observations could be tied to micro-meteorological and hydrological observations has distinct
712 advantages. These areas often have power supplies and instrumentation expertise to operate and
713 maintain disdrometer networks.

714

715 5.4 Compare different indirect phase measurement methods

716 There is an important need to evaluate the accuracy of different PPM to assess tradeoffs between
717 model complexity and skill. Given the potential for several types of observations to improve
718 precipitation phase prediction (section 5.1-5.3), quantifying the relative skill provided by these
719 different lines of evidence is a critical research gap. Although assessing relative differences
720 between methods is potentially informative, comparison to ground truth measurements is critical
721 for assessing accuracy. Disdrometer measurements are an ideal ground truth that can be
722 collected at fine time steps and under a variety of conditions (section 5.3). Less ideal for
723 accuracy assessment studies are direct visual observations that are harder to collect at fine time
724 steps and in low light conditions. Similarly, employing coupled observations of precipitation
725 and snow depth has been used to assess accuracy of different precipitation phase prediction
726 methods (Marks et al., 2013; Harder and Pomeroy, 2013), but accuracy assessment of these
727 techniques themselves are lacking under a wide range of different conditions.



728

729 A variety of accuracy assessments are needed that will require co-located distributed
730 measurements. One critical accuracy assessment involves the consistency of different
731 precipitation phase prediction methods under different climate and atmospheric conditions.
732 Assessing the effects of climate and atmospheric conditions requires measurements from a
733 variety of sites covering a range of hydroclimatic conditions and record lengths that span the
734 conceivable range of atmospheric conditions at a given site. Another important evaluation
735 metric is the performance over different time steps. Harder and Pomeroy (2013) showed that
736 hydrometeor and temperature-based prediction methods had errors that substantially decreased
737 across shorter time steps. Identifying the effects of time step length on the accuracy of different
738 prediction methods has been relatively unexplored, but is critical to selecting the proper method
739 for different hydrological applications. Finally, the performance metrics used to assess accuracy
740 should be carefully considered. The applications of precipitation phase prediction methods are
741 diverse, necessitating a wide variety of performance metrics, including the probability of snow
742 versus rain (Dai, 2008), the error in annual or total snow/rain accumulation (Rajagopal and
743 Harpold, 2016), performance under extreme conditions of precipitation amount and intensity,
744 determination of the snow-rain elevation (Marks et al., 2013), and uncertainty arising from
745 measurement error and accuracy. Comparison of different metrics across a wide-variety of sites
746 and conditions is lacking but is greatly needed to advance cold-region hydrologic science.

747

748 5.5 Develop spatially resolved products

749 Many hydrological applications will benefit from gridded data products that are easily integrated
750 into standard hydrological models. Currently, very few options exist for gridded data
751 precipitation phase products. Instead, most hydrological models have some type of submodel or
752 simple scheme that specifies precipitation phase as rain, snow, or mixed (see Section 4). While
753 testing PPM with ground based observations could lead to improved submodels, we believe
754 development of gridded forcing data may be an easier and more effective solution for many
755 hydrological modeling applications.

756

757 Gridded data products could be derived from a combination of remote sensing and existing
758 model products, but would need to be extensively evaluated. The NASA GPM mission is



759 beginning to produce gridded precipitation phase products at 3-hour and 0.1 degree resolution.
760 However, GPM phase is measured at the top of the atmosphere, typically relies on simple
761 temperature-thresholds, and is yet to be validated with ground based observations. Another
762 existing product is the Snow Data Assimilation System (SNODAS) that estimates liquid and
763 solid precipitation at the 1 km scale. However, the developers of SNODAS caution that it is not
764 suitable for estimating storm totals or regional differences. Furthermore, to our knowledge the
765 precipitation phase product from SNODAS has not been validated with ground observations.
766 We suggest the development of new gridded data products that utilize new PPM (i.e. Harder and
767 Pomeroy, 2013) and new and expanded observational datasets, such as atmospheric information
768 and radar estimates. We advocate for the development of multiple gridded products that can be
769 evaluated with ground observations to compare and contrast their strengths. This would also
770 allow for ensembles of phase estimates to be used in hydrological models, similar to what is
771 currently being done with gridded precipitation estimates.

772

773 5.6 Characterization of regional variability

774 The inclusion of new datasets, better validation of PPM, and development of gridded data
775 products will poise the hydrologic community to better quantify regional sensitivity of phase
776 change to climate changes. Because the techniques applied to assess regional variability have
777 relied on temperature (Klos et al., 2014; Knowles et al., 2006), we have not fully considered the
778 role of wet bulb depressions and humidity in our assessment of sensitivity to changes in phase.
779 Consequently, the effects of changes from snow to rain from regional warming and
780 corresponding changes in humidity will be difficult to predict with the current PPM. Recent
781 efforts by Rajagopal and Harpold (2016) have demonstrated that simple temperature thresholds
782 are insufficient to characterize snow-rain transition across the Western U.S. (Figure 3), perhaps
783 because of differences in humidity.

784

785 This local to sub-regional characterization is needed for water resource prediction and to better
786 inform decision and policy makers. In particular, the ability to predict the transitional rain-snow
787 elevations and its uncertainty is critical information for a variety of end-users, including state and
788 municipal water agencies, agricultural water boards, transportation agencies, and wildlife, forest,



789 and land managers. Fundamental advancements in characterizing regional variability are
790 possible by addressing the research challenges detailed in sections 5.1-5.5.

791

792 6. Conclusions

793 This review paper is a step towards communicating the potential bottlenecks in hydrological
794 modeling caused by poor representation of precipitation phase (Figure 1). Our goals were to
795 demonstrate that major research gaps in our ability to PPM are contributing to error and reducing
796 predictive skill in hydrological modeling. By highlighting the research gaps that could advance
797 the science of PPM, we have provided a roadmap for future advances (Figure 4). While many of
798 the research gaps are recognized by the community and are being pursued, including
799 incorporating atmospheric and humidity information, while others remain essentially unexplored
800 (e.g. production of gridded data, widespread ground validation, and remote sensing validation).

801

802 The key points that must be communicated to the hydrologic community and its funding
803 agencies can be distilled into the following two statements: 1) Current PPM algorithms are too
804 simple and are not well-validated for most locations, 2) the lack of sophisticated PPM increases
805 the uncertainty in estimation of hydrological sensitivity to changes in precipitation phase at local
806 to regional scales. We advocate for better incorporation of new information (5.1-5.2) and
807 improved validation methods (5.3-5.4) to advance our current PPM methods. These improved
808 PPM algorithms will be capable of developing gridded datasets (5.5) and providing new insight
809 that reduce the uncertainty of predicting regional changes from snow to rain (5.6). A concerted
810 effort by the hydrological and atmospheric science communities to address the PPM challenge
811 will remedy current limitations in hydrological modeling of precipitation phase, advance of
812 understanding of cold regions hydrology, and provide better information to decision makers.

813

814 Acknowledgements

815 This work was conducted as a part of an Innovation Working Group supported by the Idaho,
816 Nevada, and New Mexico EPSCoR Programs and by the National Science Foundation under
817 award numbers IIA-1329469, IIA-1329470 and IIA-1329513. Adrian Harpold was partially
818 supported by USDA NIFA NEV05293. Adrian Harpold and Rina Schumer were supported by
819 the NASA EPSCoR Cooperative Agreement #NNX14AN24A. Seshadri Rajagopal was
820 partially supported by research supported by NSF/USDA grant (#1360506/#1360507) and



821 startup funds provided by Desert Research Institute.



822 **References:**

- 823 Abatzoglou, J. T.: Development of gridded surface meteorological data for ecological
824 applications and modelling, *International Journal of Climatology*, 33, 121-131,
825 10.1002/joc.3413, 2013.
- 826 Anderson, E., 2006, Snow Accumulation and Ablation Model – Snow-17, available online at
827 http://www.nws.noaa.gov/oh/hrl/nwsrfs/users_manual/part2/_pdf/22snow17.pdf, accessed
828 August, 2016.
- 829 Arkin, P. A., and Ardanuy, P. E.: Estimating climatic-scale precipitation from space: a review, *J.*
830 *Climate*, 2, 1229-1238, 1989.
- 831 Arnold, J.G., Kiniry, J.R., Srinivasan R., Williams, J.R, Haney, E.B., and Neitsch S.L., 2012,
832 SWAT Input/Output Documentation, Texas Water Resources Institute, TR-439, available
833 online at <http://swat.tamu.edu/media/69296/SWAT-IO-Documentation-2012.pdf>, accessed
834 August, 2016.
- 835 Bales, R. C., Molotch, N. P., Painter, T. H., Dettinger, M. D., Rice, R., and Dozier, J.: Mountain
836 hydrology of the western United States, *Water Resources Research*, 42,
837 10.1029/2005wr004387, 2006.
- 838 Barnett, T. P., Adam, J. C., and Lettenmaier, D. P.: Potential impacts of a warming climate on
839 water availability in snow-dominated regions, *Nature*, 438, 303-309, 10.1038/nature04141,
840 2005.
- 841 Battaglia, A., Rustemeier, E., Tokay, A., Blahak, U., and Simmer, C.: PARSIVEL Snow
842 Observations: A Critical Assessment, *Journal of Atmospheric and Oceanic Technology*, 27,
843 333-344, 10.1175/2009jtecha1332.1, 2010.
- 844 Berghuijs, W. R., Woods, R. A., and Hrachowitz, M.: A precipitation shift from snow towards
845 rain leads to a decrease in streamflow, *Nature Climate Change*, 4, 583-586,
846 10.1038/nclimate2246, 2014.
- 847 Bernauer, F., Hurkamp, K., Ruhm, W., and Tschiersch, J.: Snow event classification with a 2D
848 video disdrometer - A decision tree approach, *Atmospheric Research*, 172, 186-195, 2016.



- 849 Bergström, S. 1995. The HBV model. In: Singh, V.P. (Ed.) Computer Models of Watershed
850 Hydrology. Water Resources Publications, Highlands Ranch, CO., pp. 443-476.
- 851 Berris, S. N., and Harr, R. D.: Comparative snow accumulation and melt during rainfall in
852 forested and clear-cut plots in the Western Cascades of Oregon, Water Resources Research,
853 23, 135-142, 10.1029/WR023i001p00135, 1987.
- 854 Bicknell, B.R., Imhoff, J.C., Kittle, J.L., Jr., Donigian, A.S., Jr., and Johanson, R.C.,
855 Hydrological Simulation Program--Fortran, User's manual for version 11: U.S.
856 Environmental Protection Agency, National Exposure Research Laboratory, Athens, Ga.,
857 EPA/600/R-97/080, 755 p., 1997.
- 858 Boe, E. T.: Assessing Local Snow Variability Using a Network of Ultrasonic Snow Depth
859 Sensors, Master of Science in Hydrologic Sciences, Geosciences, Boise State, 2013.
- 860 Boodoo, S., Hudak, D., Donaldson, N., and Leduc, M.: Application of Dual-Polarization Radar
861 Melting-Layer Detection Algorithm, Journal of Applied Meteorology and Climatology, 49,
862 1779-1793, 10.1175/2010jamc2421.1, 2010.
- 863 Borrmann, S., and Jaenicke, R.: Application of microholography for ground-based in-situ
864 measurements in stratus cloud layers - a case study, Journal of Atmospheric and Oceanic
865 Technology, 10, 277-293, 10.1175/1520-0426(1993)010<0277:aomfgb>2.0.co;2, 1993.
- 866 Braun, L. N.: Simulation of snowmelt-runoff in lowland and lower alpine regions of Switzerland,
867 Diss. Naturwiss. ETH Zürich, Nr. 7684, 0000. Ref.: Ohmura, A.; Korref.: Vischer, D.;
868 Korref.: Lang, H., 1984.
- 869 Cao, Q., Hong, Y., Chen, S., Gourley, J. J., Zhang, J., and Kirstetter, P. E.: Snowfall
870 Detectability of NASA's CloudSat: The First Cross-Investigation of Its 2C-Snow-Profile
871 Product and National Multi-Sensor Mosaic QPE (NMQ) Snowfall Data, Progress in
872 Electromagnetics Research-Pier, 148, 55-61, 10.2528/pier14030405, 2014.
- 873 Cayan, D. R., Kammerdiener, S. A., Dettinger, M. D., Caprio, J. M., and Peterson, D. H.:
874 Changes in the onset of spring in the western United States, Bulletin of the American
875 Meteorological Society, 82, 399-415, 10.1175/1520-0477(2001)082<0399:citoos>2.3.co;2,
876 2001.



- 877 Chandrasekar, V., Keranen, R., Lim, S., and Moisseev, D.: Recent advances in classification of
878 observations from dual polarization weather radars, *Atmospheric Research*, 119, 97-111,
879 10.1016/j.atmosres.2011.08.014, 2013.
- 880 Chen, S., Gourley, J. J., Hong, Y., Cao, Q., Carr, N., Kirstetter, P.-E., Zhang, J., and Flamig, Z.:
881 Using citizen science reports to evaluate estimates of surface precipitation type, *Bulletin of*
882 *the American Meteorological Society*, 10.1175/BAMS-D-13-00247.1, 2015.
- 883 Dai, A.: Temperature and pressure dependence of the rain-snow phase transition over land and
884 ocean, *Geophysical Research Letters*, 35, 10.1029/2008gl033295, 2008.
- 885 Ding, B., Yang, K., Qin, J., Wang, L., Chen, Y., and He, X.: The dependence of precipitation
886 types on surface elevation and meteorological conditions and its parameterization, *Journal*
887 *of Hydrology*, 513, 154-163, 10.1016/j.jhydrol.2014.03.038, 2014.
- 888 Eddington, L. W.: *Satellite-Derived Moisture-Bogusing Profiles for the North Atlantic Ocean*,
889 DTIC Document, 1989.
- 890 Elmore, K. L.: The NSSL Hydrometeor Classification Algorithm in Winter Surface
891 Precipitation: Evaluation and Future Development, *Weather and Forecasting*, 26, 756-765,
892 10.1175/waf-d-10-05011.1, 2011.
- 893 Fang, X., Pomeroy, J. W., Ellis, C. R., MacDonald, M. K., DeBeer, C. M., and Brown, T.: Multi-
894 variable evaluation of hydrological model predictions for a headwater basin in the Canadian
895 Rocky Mountains, *Hydrol. Earth Syst. Sci.*, 17, 1635-1659, 10.5194/hess-17-1635-2013,
896 2013.
- 897 Fatichi, S., Vivoni, E. R., Ogden, F. L., Ivanov, V. Y., Mirus, B., Gochis, D., Downer, C. W.,
898 Camporese, M., Davison, J. H., Ebel, B., Jones, N., Kim, J., Mascaro, G., Niswonger, R.,
899 Restrepo, P., Rigon, R., Shen, C., Sulis, M., and Tarboton, D.: An overview of current
900 applications, challenges, and future trends in distributed process-based models in hydrology,
901 *Journal of Hydrology*, 537, 45-60, 2016.
- 902 Feicabrino, J., Lundberg, A., and Gustafsson, D.: Improving surface-based precipitation phase
903 determination through air mass boundary identification, *Hydrology Research*, 43, 179-191,
904 10.2166/nh.2012.060, 2012.



- 905 Feiccabrino, J., Gustafsson, D., and Lundberg, A.: Surface-based precipitation phase
906 determination methods in hydrological models, *Hydrology Research*, 44, 44-57, 2013.
- 907 Floyd, W., and Weiler, M.: Measuring snow accumulation and ablation dynamics during rain-on-
908 snow events: innovative measurement techniques, *Hydrological Processes*, 22, 4805-4812,
909 10.1002/hyp.7142, 2008.
- 910 Fritze, H., Stewart, I. T., and Pebesma, E.: Shifts in Western North American Snowmelt Runoff
911 Regimes for the Recent Warm Decades, *Journal of Hydrometeorology*, 12, 989-1006,
912 10.1175/2011jhm1360.1, 2011.
- 913 Froidurot, S., Zin, I., Hingray, B., and Gautheron, A.: Sensitivity of Precipitation Phase over the
914 Swiss Alps to Different Meteorological Variables, *Journal of Hydrometeorology*, 15, 685-
915 696, 10.1175/jhm-d-13-073.1, 2014.
- 916 Garvelmann, J., Pohl, S., and Weiler, M.: From observation to the quantification of snow
917 processes with a time-lapse camera network, *Hydrology and Earth System Sciences*, 17,
918 1415-1429, 10.5194/hess-17-1415-2013, 2013.
- 919 Giangrande, S. E., Krause, J. M., and Ryzhkov, A. V.: Automatic designation of the melting
920 layer with a polarimetric prototype of the WSR-88D radar, *Journal of Applied Meteorology*
921 and *Climatology*, 47, 1354-1364, 10.1175/2007jamc1634.1, 2008.
- 922 Gilmore, M. S., Straka, J. M., and Rasmussen, E. N.: Precipitation Uncertainty Due to Variations
923 in Precipitation Particle Parameters within a Simple Microphysics Scheme, *Monthly*
924 *Weather Review*, 132, 2610-2627, 10.1175/MWR2810.1, 2004.
- 925 Godsey, S. E., Kirchner, J. W., and Tague, C. L.: Effects of changes in winter snowpacks on
926 summer low flows: case studies in the Sierra Nevada, California, USA, *Hydrological*
927 *Processes*, 28, 5048-5064, 10.1002/hyp.9943, 2014.
- 928 Grazioli, J., Tuia, D., and Berne, A.: Hydrometeor classification from polarimetric radar
929 measurements: a clustering approach, *Atmospheric Measurement Techniques*, 8, 149-170,
930 10.5194/amt-8-149-2015, 2015.
- 931 Gusev, E.M. and Nasonova, O.N., Parameterization of Heat and Water Exchange on Land
932 Surface for Coupling Hydrologic and Climate Models, *Water Resources.*, 25(4): 421-431,
933 1998.



- 934 Harder, P., and Pomeroy, J.: Estimating precipitation phase using a psychrometric energy
935 balance method, *Hydrological Processes*, 27, 1901-1914, 10.1002/hyp.9799, 2013.
- 936 Harder, P., and Pomeroy, J. W.: Hydrological model uncertainty due to precipitation-phase
937 partitioning methods, *Hydrological Processes*, 28, 4311-4327, 2014.
- 938 Hauser, D., Amayenc, P., and Nutten, B.: A new optical instrument for simultaneous
939 measurement of raindrop diameter and fall speed distributions, *Atmos. Oceanic Technol.*, 1,
940 256-259, 1984.
- 941 HEC-1, 1998, Flood Hydrograph Package, User's Manual, CPD-1A, Version 4.1, available
942 online at,
943 [http://www.hec.usace.army.mil/publications/ComputerProgramDocumentation/HEC-](http://www.hec.usace.army.mil/publications/ComputerProgramDocumentation/HEC-1_UsersManual_(CPD-1a).pdf)
944 [1_UsersManual_\(CPD-1a\).pdf](http://www.hec.usace.army.mil/publications/ComputerProgramDocumentation/HEC-1_UsersManual_(CPD-1a).pdf), accessed August, 2016.
- 945 Hedrick, A. R., and Marshall, H.-P.: Automated Snow Depth Measurements in Avalanche
946 Terrain Using Time-Lapse Photography, 2014 International Snow Science Workshop, 2014,
- 947 Hou, A. Y., Kakar, R. K., Neeck, S., Azarbarzin, A. A., Kummerow, C. D., Kojima, M., Oki, R.,
948 Nakamura, K., and Iguchi, T.: The global precipitation measurement mission, *Bulletin of the*
949 *American Meteorological Society*, 95, 701-722, 2014.
- 950 Jepsen, S. M., Harmon, T. C., Meadows, M. W., and Hunsaker, C. T.: Hydrogeologic influence
951 on changes in snowmelt runoff with climate warming: Numerical experiments on a mid-
952 elevation catchment in the Sierra Nevada, USA, *Journal of Hydrology*, 533, 332-342,
953 10.1016/j.jhydrol.2015.12.010, 2016.
- 954 Joss, J., and Waldvogel, A.: Ein Spektograph fuer Niederschlagstropfen mit automatischer
955 Auswertung, *Pure Appl. Geophys*, 68, 240--246, 1967.
- 956 Kalnay, E., and Cai, M.: Impact of urbanization and land-use change on climate, *Nature*, 423,
957 528-531, 10.1038/nature01675, 2003.
- 958 Kaplan, M. L., Vellore, R. K., Marzette, P. J., and Lewis, J. M.: The role of windward-side
959 diabatic heating in Sierra Nevada spillover precipitation, *Journal of Hydrometeorology*, 13,
960 1172-1194, 2012.



- 961 Kidd, C.: On rainfall retrieval using polarization-corrected temperatures, *International Journal of*
962 *Remote Sensing*, 19, 981-996, 10.1080/014311698215829, 1998.
- 963 Kidd, C., and Huffman, G.: Global precipitation measurement, *Meteorological Applications*, 18,
964 334-353, 10.1002/met.284, 2011.
- 965 Kienzle, S. W.: A new temperature based method to separate rain and snow, *Hydrological*
966 *Processes*, 22, 5067-5085, 10.1002/hyp.7131, 2008.
- 967 Kim, M. J., Weinman, J. A., Olson, W. S., Chang, D. E., Skofronick-Jackson, G., and Wang, J.
968 R.: A physical model to estimate snowfall over land using AMSU-B observations, *Journal*
969 *of Geophysical Research-Atmospheres*, 113, 16, 10.1029/2007jd008589, 2008.
- 970 Kirchner, J. W.: Getting the right answers for the right reasons: Linking measurements, analyses,
971 and models to advance the science of hydrology, *Water Resources Research*, 42,
972 10.1029/2005wr004362, 2006.
- 973 Kite, G. 1995. The HBV model. In: Singh, V.P. (Ed.) *Computer Models of Watershed*
974 *Hydrology*. Water Resources Publications, Highlands Ranch, CO., pp. 443-476.
- 975 Klos, P. Z., Link, T. E., and Abatzoglou, J. T.: Extent of the rain-snow transition zone in the
976 western US under historic and projected climate, *Geophysical Research Letters*, 41, 4560-
977 4568, 10.1002/2014gl060500, 2014.
- 978 Knollenberg, R. G.: Some results of measurements of latent heat released from seeded stratus,
979 *Bulletin of the American Meteorological Society*, 51, 580-&, 1970.
- 980 Knowles, N., Dettinger, M. D., and Cayan, D. R.: Trends in snowfall versus rainfall in the
981 Western United States, *Journal of Climate*, 19, 4545-4559, 2006.
- 982 Kongoli, C., Pellegrino, P., Ferraro, R. R., Grody, N. C., and Meng, H.: A new snowfall
983 detection algorithm over land using measurements from the Advanced Microwave Sounding
984 Unit (AMSU), *Geophysical Research Letters*, 30, 10.1029/2003gl017177, 2003.
- 985 Kongoli, C., Meng, H., Dong, J., and Ferraro, R.: A snowfall detection algorithm over land
986 utilizing high-frequency passive microwave measurements-Application to ATMS, *Journal*
987 *of Geophysical Research-Atmospheres*, 120, 1918-1932, 10.1002/2014jd022427, 2015.



- 988 Kruger, A., and Krajewski, W. F.: Two-dimensional video disdrometer: A description, *Journal of*
989 *Atmospheric and Oceanic Technology*, 19, 602-617, 10.1175/1520-
990 0426(2002)019<0602:tdvdad>2.0.co;2, 2002.
- 991 Kulie, M. S., Milani, L., Wood, N. B., Tushaus, S. A., Bennartz, R., and L'Ecuyer, T. S.: A
992 Shallow Cumuliform Snowfall Census Using Spaceborne Radar, *Journal of*
993 *Hydrometeorology*, 17, 1261-1279, 10.1175/jhm-d-15-0123.1, 2016.
- 994 L'hôte, Y., Chevallier, P., Coudrain, A., Lejeune, Y., and Etchevers, P.: Relationship between
995 precipitation phase and air temperature: comparison between the Bolivian Andes and the
996 Swiss Alps/Relation entre phase de précipitation et température de l'air: comparaison entre
997 les Andes Boliviennes et les Alpes Suisses, *Hydrological sciences journal*, 50, 2005.
- 998 Leavesley, G. H., Restrepo, P. J., Markstrom, S. L., Dixon, M., and Stannard, L. G.: The
999 Modular Modeling System (MMS): User's Manual, U.S. Geological Survey, Denver,
1000 COOpen File Report 96-151, 1996.
- 1001 Lempio, G. E., Bumke, K., and Macke, A.: Measurement of solid precipitation with an optical
1002 disdrometer, *Advances in Geosciences*, 10, 91-97, 2007.
- 1003 Lewis, J., Lakshminarayanan, S., and Dhall, S.: *Dynamic Data Assimilation: A Least Squares*
1004 *Approach*, Cambridge Univ. Press, 745 pp., 2006.
- 1005 Lin, Y.-L.: *Mesoscale Dynamics*, Cambridge University Press, 630 pp., 2007.
- 1006 Liu, G.: Deriving snow cloud characteristics from CloudSat observations, *Journal of Geophysical*
1007 *Research-Atmospheres*, 113, 10.1029/2007jd009766, 2008.
- 1008 Loffler-Mang, M., Kunz, M., and Schmid, W.: On the performance of a low-cost K-band
1009 Doppler radar for quantitative rain measurements, *Journal of Atmospheric and Oceanic*
1010 *Technology*, 16, 379-387, 10.1175/1520-0426(1999)016<0379:otpoal>2.0.co;2, 1999.
- 1011 Luce, C. H., and Holden, Z. A.: Declining annual streamflow distributions in the Pacific
1012 Northwest United States, 1948-2006, *Geophysical Research Letters*, 36,
1013 10.1029/2009gl039407, 2009.
- 1014 Lundquist, J. D., Neiman, P. J., Martner, B., White, A. B., Gattas, D. J., and Ralph, F. M.: Rain
1015 versus snow in the Sierra Nevada, California: Comparing Doppler profiling radar and



- 1016 surface observations of melting level, *Journal of Hydrometeorology*, 9, 194-211,
1017 10.1175/2007jhm853.1, 2008.
- 1018 Lynch-Stieglitz, M.: The development and validation of a simple snow model for the GISS
1019 GCM, *Journal of Climate*, 7, 1842-1855, 1994.
- 1020 Marks, D., Link, T., Winstral, A., and Garen, D.: Simulating snowmelt processes during rain-on-
1021 snow over a semi-arid mountain basin, *Annals of Glaciology*, 32, 195-202, 2001.
- 1022 Marks, D., Winstral, A., Reba, M., Pomeroy, J., and Kumar, M.: An evaluation of methods for
1023 determining during-storm precipitation phase and the rain/snow transition elevation at the
1024 surface in a mountain basin, *Advances in Water Resources*, 55, 98-110,
1025 <http://dx.doi.org/10.1016/j.advwatres.2012.11.012>, 2013.
- 1026 Martinec, J., and Rango, A.: Parameter values for snowmelt runoff modelling, *Journal of*
1027 *Hydrology*, 84, 197-219, [http://dx.doi.org/10.1016/0022-1694\(86\)90123-X](http://dx.doi.org/10.1016/0022-1694(86)90123-X), 1986.
- 1028 Martinec J., Rango A., Roberts R., 2008, Snowmelt Runoff Model, User's Manual, available
1029 online at http://aces.nmsu.edu/pubs/research/weather_climate/SRMSpecRep100.pdf,
1030 accessed August, 2016.
- 1031 Matrosov, S. Y., Shupe, M. D., and Djalalova, I. V.: Snowfall retrievals using millimeter-
1032 wavelength cloud radars, *Journal of Applied Meteorology and Climatology*, 47, 769-777,
1033 10.1175/2007jamc1768.1, 2008.
- 1034 Maurer, E. P., and Mass, C.: Using radar data to partition precipitation into rain and snow in a
1035 hydrologic model, *Journal of Hydrologic Engineering*, 11, 214-221, 10.1061/(asce)1084-
1036 0699(2006)11:3(214), 2006.
- 1037 McCabe, G. J., and Wolock, D. M.: General-circulation-model simulations of future snowpack in
1038 the western United States1. *JAWRA Journal of the American Water Resources Association*,
1039 35(6), 1473-1484, 1999.
- 1040 McCabe, G.J. and Wolock, D.M.: Recent Declines in Western U.S. Snowpack in the Context of
1041 Twentieth-Century Climate Variability, *Earth Interactions*, 13, 1-15, DOI:
1042 10.1175/2009EI283.1, 1999.



- 1043 McCabe, G. J., Clark, M. P., and Hay, L. E.: Rain-on-snow events in the western United States,
1044 Bulletin of the American Meteorological Society, 88, 319-+, 10.1175/bams-88-3-319, 2007.
- 1045 McCabe, G. J., and Wolock, D. M.: Long-term variability in Northern Hemisphere snow cover
1046 and associations with warmer winters, Climatic Change, 99, 141-153, 2010.
- 1047 MIKE-SHE User Manual, available online at
1048 ftp://ftp.cgs.si/Uporabniki/UrosZ/mike/Manuals/MIKE_SHE/MIKE_SHE.htm, accessed
1049 August, 2016.
- 1050 Milly, P. C. D., Betancourt, J., Falkenmark, M., Hirsch, R. M., Kundzewicz, Z. W., Lettenmaier,
1051 D. P., and Stouffer, R. J.: Climate change - Stationarity is dead: Whither water
1052 management?, Science, 319, 573-574, 10.1126/science.1151915, 2008.
- 1053 Minder, J. R.: The Sensitivity of Mountain Snowpack Accumulation to Climate Warming,
1054 Journal of Climate, 23, 2634-2650, 10.1175/2009jcli3263.1, 2010.
- 1055 Minder, J. R., and Kingsmill, D. E.: Mesoscale Variations of the Atmospheric Snow Line over
1056 the Northern Sierra Nevada: Multiyear Statistics, Case Study, and Mechanisms, Journal of
1057 the Atmospheric Sciences, 70, 916-938, 10.1175/jas-d-12-0194.1, 2013.
- 1058 Mitchell K., Ek, M., Wong, V., Lohmann, D., Koren, V., Schaake, J., Duan, Q., Gayno, G.,
1059 Moore, B., Grunmann, P., Tarpley, D., Ramsay, B., Chen, F., Kim, J., Pan, H.L., Lin, Y.,
1060 Marshall, C., Mahrt, L., Meyers, T., and Ruscher, P.: 2005, Noah Land-Surface Model,
1061 User's Guide, version 2.7.1, available at
1062 ftp://ftp.emc.ncep.noaa.gov/mmb/gcp/ldas/noahism/ver_2.7.1, accessed August, 2016.
- 1063 Mizukami, N., Koren, V., Smith, M., Kingsmill, D., Zhang, Z. Y., Cosgrove, B., and Cui, Z. T.:
1064 The Impact of Precipitation Type Discrimination on Hydrologic Simulation: Rain-Snow
1065 Partitioning Derived from HMT-West Radar-Detected Brightband Height versus Surface
1066 Temperature Data, Journal of Hydrometeorology, 14, 1139-1158, 10.1175/jhm-d-12-035.1,
1067 2013.
- 1068 Morrison, H., Curry, J., and Khvorostyanov, V.: A new double-moment microphysics
1069 parameterization for application in cloud and climate models. Part I: Description, Journal of
1070 the Atmospheric Sciences, 62, 1665-1677, 2005.



- 1071 Motoyama, H.: Simulation of seasonal snowcover based on air temperature and precipitation,
1072 *Journal of Applied Meteorology*, 29, 1104-1110, 1990.
- 1073 Noh, Y. J., Liu, G. S., Jones, A. S., and Haar, T. H. V.: Toward snowfall retrieval over land by
1074 combining satellite and in situ measurements, *Journal of Geophysical Research-*
1075 *Atmospheres*, 114, 10.1029/2009jd012307, 2009.
- 1076 Olsen, A.: Snow or rain?—A matter of wet-bulb temperature, thesis, Uppsala Univ., Uppsala,
1077 Sweden.(Available at [http://www. geo. uu. se/luva/exarb/2003/Arvid_Olsen. pdf](http://www.geo.uu.se/luva/exarb/2003/Arvid_Olsen.pdf)), 2003.
- 1078 Olson, W. S., Kummerow, C. D., Heymsfield, G. M., and Giglio, L.: A method for combined
1079 passive-active microwave retrievals of cloud and precipitation profiles, *Journal of Applied*
1080 *Meteorology*, 35, 1763-1789, 10.1175/1520-0450(1996)035<1763:amfcpm>2.0.co;2, 1996.
- 1081 Pachauri, R. K.: Intergovernmental panel on climate change (IPCC): Keynote address,
1082 *Environmental Science and Pollution Research*, 9, 436-438, 2002.
- 1083 Pagano, T. C., Wood, A. W., Ramos, M. H., Cloke, H. L., Pappenberger, F., Clark, M. P.,
1084 Cranston, M., Kavetski, D., Mathevet, T., Sorooshian, S., and Verkade, J. S.: Challenges of
1085 Operational River Forecasting, *Journal of Hydrometeorology*, 15, 1692-1707, 10.1175/jhm-
1086 d-13-0188.1, 2014.
- 1087 Parajka, J., Haas, P., Kirnbauer, R., Jansa, J., and Bloeschl, G.: Potential of time-lapse
1088 photography of snow for hydrological purposes at the small catchment scale, *Hydrological*
1089 *Processes*, 26, 3327-3337, 10.1002/hyp.8389, 2012.
- 1090 Park, H., Ryzhkov, A. V., Zrnica, D. S., and Kim, K.-E.: The Hydrometeor Classification
1091 Algorithm for the Polarimetric WSR-88D: Description and Application to an MCS, *Weather*
1092 *and Forecasting*, 24, 730-748, 10.1175/2008waf2222205.1, 2009.
- 1093 Pipes, A., and Quick, M. C.: UBC watershed model users guide, Department of Civil
1094 Engineering, University of British Columbia, 1977.
- 1095 Rajagopal, S., and Harpold, A.: Testing and Improving Temperature Thresholds for Snow and
1096 Rain Prediction in the Western United States, *Journal of American Water Resources*
1097 *Association*, 2016.



- 1098 Rasmussen, R., Baker, B., Kochendorfer, J., Meyers, T., Landolt, S., Fischer, A. P., Black, J.,
1099 Thériault, J. M., Kucera, P., Gochis, D., Smith, C., Nitu, R., Hall, M., Ikeda, K., and
1100 Gutmann, E.: How Well Are We Measuring Snow: The NOAA/FAA/NCAR Winter
1101 Precipitation Test Bed, *Bulletin of the American Meteorological Society*, 93, 811-829,
1102 10.1175/BAMS-D-11-00052.1, 2012.
- 1103 Reisner, J., Rasmussen, R. M., and Bruintjes, R.: Explicit forecasting of supercooled liquid water
1104 in winter storms using the MM5 mesoscale model, *Quarterly Journal of the Royal
1105 Meteorological Society*, 124, 1071-1107, 1998.
- 1106 Rojas, R., Feyen, L., Dosio, A., and Bavera, D.: Improving pan-European hydrological
1107 simulation of extreme events through statistical bias correction of RCM-driven
1108 climate simulations, *Hydrology and Earth System Sciences*, 15, 2599, 2011.
- 1109 Safeeq, M., Mauger, G. S., Grant, G. E., Arismendi, I., Hamlet, A. F., and Lee, S. Y.: Comparing
1110 Large-Scale Hydrological Model Predictions with Observed Streamflow in the Pacific
1111 Northwest: Effects of Climate and Groundwater, *Journal of Hydrometeorology*, 15, 2501-
1112 2521, 10.1175/jhm-d-13-0198.1, 2014.
- 1113 Sevruk, B.: Assessment of snowfall proportion in monthly precipitation in Switzerland, *Zbornik
1114 meteoroloskih i Hidroloskih Radovav Beograd*, 10, 315-318, 1984.
- 1115 Shamir, E., and Georgakakos, K. P.: Distributed snow accumulation and ablation modeling in the
1116 American River basin, *Advances in Water Resources*, 29, 558-570,
1117 10.1016/j.advwatres.2005.06.010, 2006.
- 1118 Skamarock, W. C., Klemp, J. B., Dudhia, J., Gill, D. O., Barker, D. M., Duda, M. G., Huang, X.-
1119 Y., Wang, W., and Powers, J. G.: A description of the advanced research WRF version
1120 3NCAR Tech. Note NCAR/TN-475+STR, 113, 2008.
- 1121 Skofronick-Jackson, G., Hudak, D., Petersen, W., Nesbitt, S. W., Chandrasekar, V., Durden, S.,
1122 Gleicher, K. J., Huang, G.-J., Joe, P., Kollias, P., Reed, K. A., Schwaller, M. R., Stewart, R.,
1123 Tanelli, S., Tokay, A., Wang, J. R., and Wolde, M.: Global Precipitation Measurement Cold
1124 Season Precipitation Experiment (GCPEX): For Measurement's Sake, Let It Snow, *Bulletin
1125 of the American Meteorological Society*, 96, 1719-1741, doi:10.1175/BAMS-D-13-00262.1,
1126 2015.



- 1127 SNTHERM Online Documentation, available at
1128 <http://www.geo.utexas.edu/climate/Research/SNOWMIP/SUPERSNOW2/rjordan.html>,
1129 accessed August, 2016.
- 1130 Stewart, R. E.: Precipitation Types in the Transition Region of Winter Storms, Bulletin of the
1131 American Meteorological Society, 73, 287-296, 10.1175/1520-
1132 0477(1992)073<0287:PTITTR>2.0.CO;2, 1992.
- 1133 Stewart, R. E., Theriault, J. M., and Henson, W.: On the Characteristics of and Processes
1134 Producing Winter Precipitation Types near 0 degrees C, Bulletin of the American
1135 Meteorological Society, 96, 623-639, 10.1175/bams-d-14-00032.1, 2015.
- 1136 Tague, C.L, and Band, L.E.: RHESSys: Regional Hydro-Ecologic Simulation System—An
1137 Object Oriented Approach to Spatially Distributed Modeling of Carbon, Water, and Nutrient
1138 Cycling, Earth Interactions, 8, 19, 1-42, 2004.
- 1139 Tarboton, D.G., and Luce, C.H., 1996, Utah Energy Balance Snow Accumulation and Melt
1140 Model (UEB), available online at
1141 http://www.fs.fed.us/rm/boise/publications/watershed/rmrs_1996_tarbotond001.pdf,
1142 accessed August, 2016.
- 1143 Tarboton, D., Jackson, T., Liu, J., Neale, C., Cooley, K., and McDonnell, J.: A Grid Based
1144 Distributed Hydrologic Model: Testing Against Data from Reynolds Creek Experimental
1145 Watershed, Preprints AMS Conf. on Hydrol, 79-84, 1995.
- 1146 Theriault, J. M., and Stewart, R. E.: On the effects of vertical air velocity on winter precipitation
1147 types, Natural Hazards and Earth System Sciences, 7, 231-242, 2007.
- 1148 Theriault, J. M., and Stewart, R. E.: A Parameterization of the Microphysical Processes Forming
1149 Many Types of Winter Precipitation, Journal of the Atmospheric Sciences, 67, 1492-1508,
1150 10.1175/2009jas3224.1, 2010.
- 1151 Theriault, J. M., Stewart, R. E., and Henson, W.: On the Dependence of Winter Precipitation
1152 Types on Temperature, Precipitation Rate, and Associated Features, Journal of Applied
1153 Meteorology and Climatology, 49, 1429-1442, 10.1175/2010jamc2321.1, 2010.



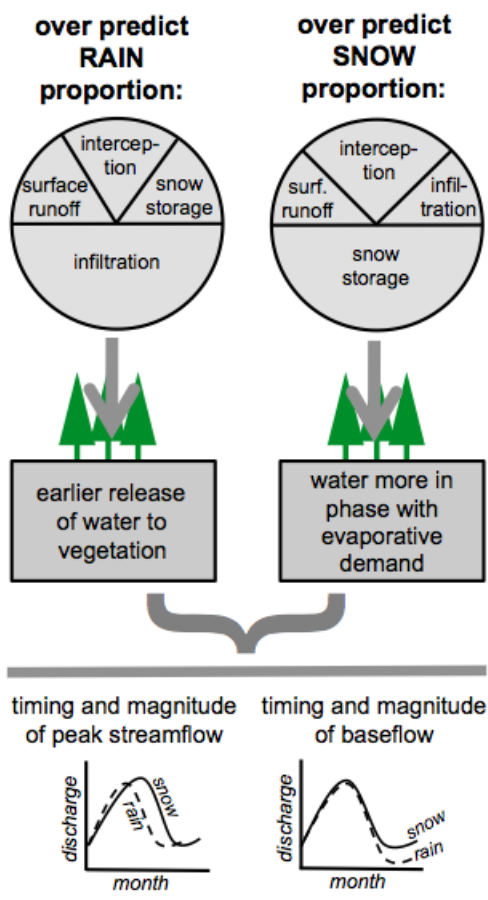
- 1154 Theriault, J. M., Stewart, R. E., and Henson, W.: Impacts of terminal velocity on the trajectory of
1155 winter precipitation types, *Atmospheric Research*, 116, 116-129,
1156 10.1016/j.atmosres.2012.03.008, 2012.
- 1157 Thompson, E. J., Rutledge, S. A., Dolan, B., Chandrasekar, V., and Cheong, B. L.: A Dual-
1158 Polarization Radar Hydrometeor Classification Algorithm for Winter Precipitation, *Journal*
1159 *of Atmospheric and Oceanic Technology*, 31, 1457-1481, 10.1175/jtech-d-13-00119.1,
1160 2014.
- 1161 Thompson, G., Rasmussen, R. M., and Manning, K.: Explicit forecasts of winter precipitation
1162 using an improved bulk microphysics scheme. Part I: Description and sensitivity analysis,
1163 *Monthly Weather Review*, 132, 519-542, 2004.
- 1164 Thompson, G., Field, P. R., Rasmussen, R. M., and Hall, W. D.: Explicit forecasts of winter
1165 precipitation using an improved bulk microphysics scheme. Part II: Implementation of a
1166 new snow parameterization, *Monthly Weather Review*, 136, 5095-5115, 2008.
- 1167 Todini, E.: The ARNO Rainfall-runoff model, *Journal of Hydrology*, 175, 339-382, 1996.
- 1168 Tung, C.-P., and Haith, D. A.: Global-warming effects on New York streamflows, *Journal of*
1169 *Water Resources Planning and Management*, 121, 216-225, 1995.
- 1170 U.S. Army Corps of Engineers: Summary Report of the Snow Investigation Hydrological
1171 Practices,” 3rd Edition, Chapter 2, North Pacific Division, Portland, Oregon,, 1956.
- 1172 Versegny, D., 2009, CLASS-The Canadian Land Surface Scheme, Version 3.4, Technical
1173 Documentation, Version 1.1, Environment Canada, available online at
1174 http://www.usask.ca/ip3/download/CLASS_v3_4_Documentation_v1_1.pdf, accessed
1175 August, 2016.
- 1176 VIC Documentation, available online at <https://vic.readthedocs.io/en/develop/>, accessed August,
1177 2016.
- 1178 Wang, R., Kumar, M., and Link, T. E.: Potential Trends in Snowmelt Generated Peak
1179 Streamflows in a Warming Climate, *Geophys. Res. Lett.* , NEED PUBLICATION INFO,
1180 2016.



- 1181 Wen, L., Nagabhatla, N., Lu, S., and Wang, S.-Y.: Impact of rain snow threshold temperature on
1182 snow depth simulation in land surface and regional atmospheric models, *Advances in*
1183 *Atmospheric Sciences*, 30, 1449-1460, 10.1007/s00376-012-2192-7, 2013.
- 1184 White, A. B., Gottas, D. J., Strem, E. T., Ralph, F. M., and Neiman, P. J.: An automated
1185 brightband height detection algorithm for use with Doppler radar spectral moments, *Journal*
1186 *of Atmospheric and Oceanic Technology*, 19, 687-697, 10.1175/1520-
1187 0426(2002)019<0687:aabhda>2.0.co;2, 2002.
- 1188 White, A. B., Gottas, D. J., Henkel, A. F., Neiman, P. J., Ralph, F. M., and Gutman, S. I.:
1189 Developing a Performance Measure for Snow-Level Forecasts, *Journal of*
1190 *Hydrometeorology*, 11, 739-753, 10.1175/2009jhm1181.1, 2010.
- 1191 Wigmosta, M.S., Vail, L.W., and Lettenmaier, D.P.: A distributed hydrology-vegetation model
1192 for complex terrain, *Water Resources Research*, 30(6), 1665-1679, 1994.
- 1193 Wilheit, T. T., Chang, A. T. C., King, J. L., Rodgers, E. B., Nieman, R. A., Krupp, B. M.,
1194 Milman, A. S., Stratigos, J. S., and Siddalingaiah, H.: Microwave radiometric observation
1195 near 19.35, 92 and 183 GHz of precipitation in tropical storm Cora, *Journal of Applied*
1196 *Meteorology*, 21, 1137-1145, 10.1175/1520-0450(1982)021<1137:mronag>2.0.co;2, 1982.
- 1197 Wood, A. W., Leung, L. R., Sridhar, V., and Lettenmaier, D.: Hydrologic implications of
1198 dynamical and statistical approaches to downscaling climate model outputs, *Climatic*
1199 *change*, 62, 189-216, 2004.
- 1200 Wood, N., L'Ecuyer, T. S., Vane, D., Stephens, G., and Partain, P.: Level 2C snow profile
1201 process description and interface control document, 2013.
- 1202 Yamazaki, T.: A One-dimensional Land Surface Model Adaptable to Intensely Cold Regions and
1203 its Applications in Eastern Siberia, 79, 1107-1118, 2001.
- 1204 Yang Z.L., Dickinson, R.E., Robock, A. and Vinniko, K.Y.: Validation of the Snow Submodel of
1205 the Biosphere–Atmosphere Transfer Scheme with Russian Snow Cover and Meteorological
1206 Observational Data, *J. Climate*, 10, 353–373, doi: 10.1175/1520-
1207 0442(1997)010<0353:VOTSSO>2.0.CO;2, 1997.
- 1208 Yarnell, S. M., Viers, J. H., and Mount, J. F.: Ecology and Management of the Spring Snowmelt
1209 Recession, *Bioscience*, 60, 114-127, 10.1525/bio.2010.60.2.6, 2010.



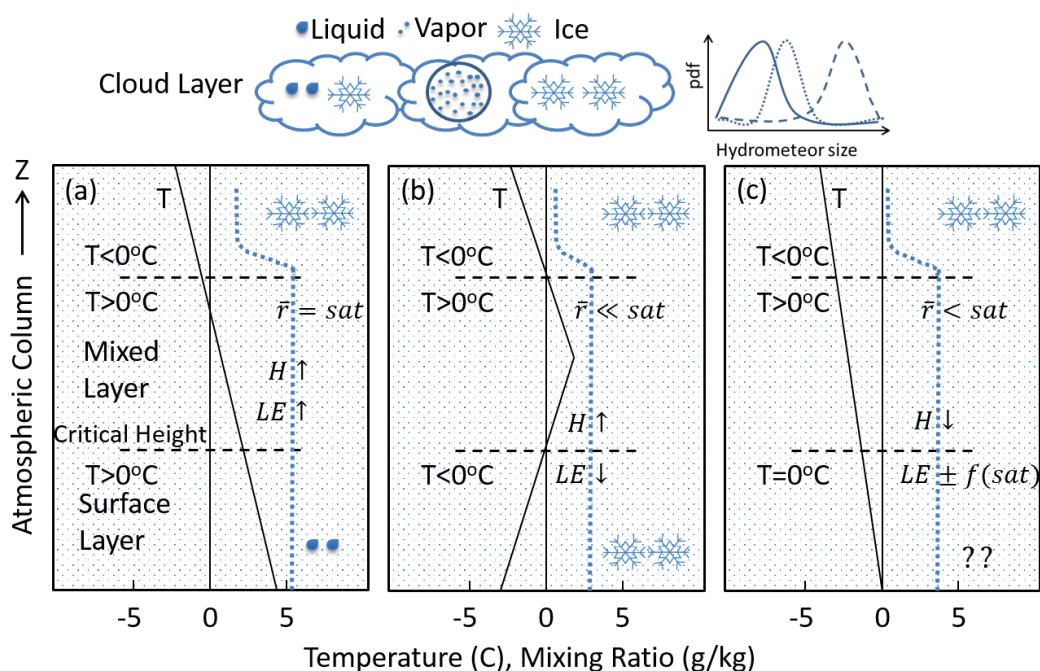
- 1210 Ye, H., Cohen, J., and Rawlins, M.: Discrimination of Solid from Liquid Precipitation over
1211 Northern Eurasia Using Surface Atmospheric Conditions, *Journal of Hydrometeorology*, 14,
1212 1345-1355, 2013a.
- 1213 Ye, H., Cohen, J., and Rawlins, M.: Discrimination of Solid from Liquid Precipitation over
1214 Northern Eurasia Using Surface Atmospheric Conditions, *Journal of Hydrometeorology*, 14,
1215 1345-1355, 10.1175/jhm-d-12-0164.1, 2013b.
- 1216 Yucel, I., Onen, A., Yilmaz, K. K., and Gochis, D. J.: Calibration and evaluation of a flood
1217 forecasting system: Utility of numerical weather prediction model, data assimilate, and
1218 satellite-based rainfall, *Journal of Hydrology*, 523, 49-66, 10.1016/j.hydro.2015.01.042,
1219 2015.
- 1220 Zängl, G.: Interaction between dynamics and cloud microphysics in orographic precipitation
1221 enhancement: A high-resolution modeling study of two North Alpine heavy-precipitation
1222 events, *Monthly weather review*, 135, 2817-2840, 2007.
- 1223 Zanotti, F., Endrizzi, S., Bertoldi, G. and Rigon, R.: The GEOTOP snow module, *Hydrological*
1224 *Processes*, 18, 3667–3679. doi:10.1002/hyp.5794, 2004.
- 1225
- 1226
- 1227



1228

1229 **Figure 1.** Precipitation phase has numerous implications for modeling the magnitude, storage,
1230 partitioning, and timing of water inputs and outputs. Potentially affecting important
1231 ecohydrological and streamflow quantities important for prediction.

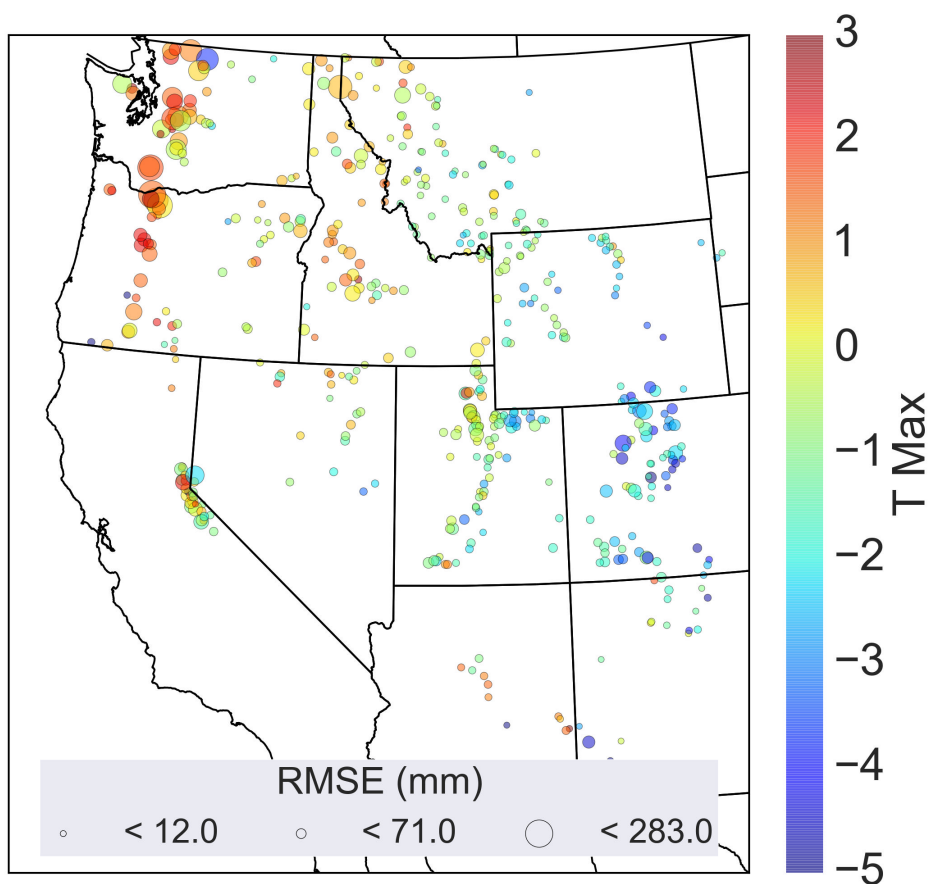
1232



1233

1234 Figure 2: The phase of precipitation at the ground surface is strongly controlled by atmospheric
 1235 profiles of temperature and humidity. While conditions exist that are relatively easy to predict
 1236 rain (a) and snow (b), many conditions lead to complex heat exchanges that are difficult to
 1237 predict with ground based observations alone (c).

1238



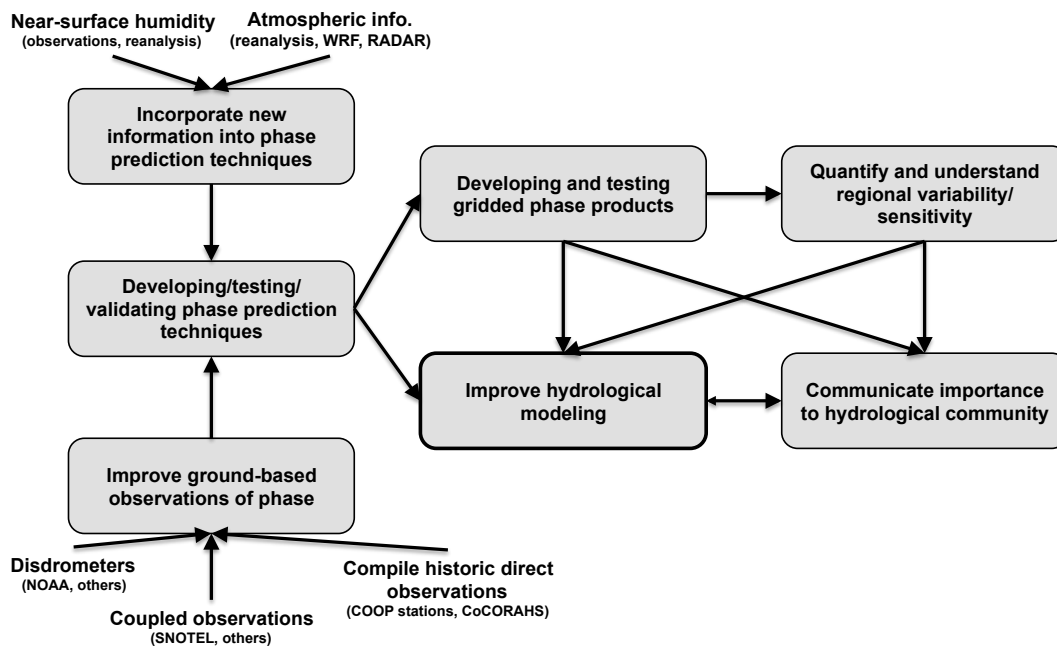
1239

1240 Figure 3. The optimized critical maximum daily temperature threshold that produced the lowest
1241 Root Mean Square Error (RMSE) in the prediction of snowfall at Snow Telemetry (SNOTEL)
1242 stations across the western US (adapted from Rajagopal and Harpold, 2016).



1243

1244



1245

1246 Figure 4. Conceptual representation of the research gaps and workflows needed to advance PPM
1247 and improve hydrological modeling.

1248



1249 Table 1. Common hydrological models and the precipitation phase prediction (PPM) technique
 1250 employed. The citation referring to the original publication of the model is given.

Model	PPM technique	Citations
<u>Discrete Models (not coupled)</u>		
HBV	Static Threshold	Bergström, 1995
Snowmelt Runoff Model	Static Threshold	Martinec et al., 2008
SLURP	Static Threshold	Kite, 1995
UBC Watershed Model	Linear Transition	Pipes and Quick, 1977
PRMS model	Minimum & Maximum Temperature	Leavesley et al., 1996
USGS water budget	Linear transition between two mean temps	McCabe and Wolock, 2009
SAC-SMA (SNOW-17)	Static Threshold	Anderson, 2006
DHSVM	Linear transition (double check)	Wigmosta et al., 1994
SWAT	Threshold Model	Arnold et al., 2012
RHESSys	Linear transition or input phase	Tague and Band, 2004
HSPF	Air and dew point temperature thresholds	Bicknell et al., 1997
THE ARNO MODEL	Static Threshold	Todini, 1996
HEC-1	Static Threshold	HEC-1, 1998
MIKE SHE	Static Threshold	MIKE-SHE User Manual
SWAP	Static Threshold	Gusev and Nasonova, 1998
BATS	Static Threshold	Yang et al., 1997
Utah Energy Balance	Linear Transition	Tarboton and Luce, 1996
SNOBAL/ISNOBAL	Linear Transition*	Marks et al., 2013
CRHM	Static Threshold	Fang et al., 2013
GEOTOP	Linear Transition	Zanotti et al. 2004
SNTHERM	Linear Transition	SNTHERM Online Documentation
<u>Offline LS models</u>		
Noah	Static Threshold	Mitchell et al., 2005
VIC	Static Threshold	VIC Documentation
CLASS	Multiple Methods ⁺	Versegny, 2009

1251

1252 * by default. Temperature-phase-density relationship explicitly specified by user.

1253 + A flag is specified which switches between, static threshold, linear transition.

1254